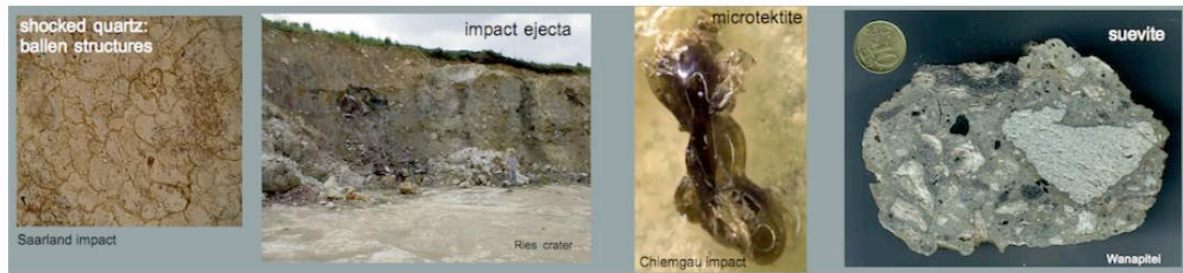


ERNSTSON CLAUDIN IMPACT STRUCTURES – METEORITE CRATERS

Research on impact geology, geophysics, petrology, and impact cratering



ARTICLE (August 2019)

New approach to an old debate: The Pelarda Formation meteorite impact ejecta (Azulara structure, Iberian Chain, NE Spain)

Ferran Claudin¹, Kord Ernstson², Wolfgang Monninger³

Abstract. - The Pelarda Formation (Fm.), located in the Iberian System in northeast Spain, is a sedimentary deposit with an extension of roughly 12 km x 2.5 km and an estimated thickness of no more than 400 m. The formation was first recognized as a peculiar unit in the early seventies and underwent interpretations like a fluvial or an alluvial fan deposit having a postulated age between Paleogene and Quaternary. Since the early nineties the Pelarda Formation has been considered an impact ejecta deposit originating from the large ca. 40 km-diameter Azulara impact structure and meanwhile being among the largest and most prominent terrestrial impact ejecta occurrences, which however is questioned by regional geologists still defending the fluvial and alluvial fan models. Roughly speaking, the Pelarda Fm. is a grossly unsorted, matrix-supported diamictite with grain sizes between silt fraction and meter-sized clasts and a big intercalated megablock. Strong clast deformations and abundant shock metamorphic effects like planar deformation features (PDF) are observed throughout the Pelarda F. deposit compatible with its impact ejecta origin. Aligned bigger clasts and smaller intercalated bands of sandstones, siltstones and clayey material indicate some local stratification obviously adjusted to flow processes within the impact ejecta curtain. This suggests that gravitational flows predominated in a transport by water in both liquid and gas states. Transport and deposition as a kind of pyroclastic surge are discussed. A sketch sequence describes the emplacement process of the Pelarda Fm. as

part of the Azuara crater formation and the integration in the general frame of pre-impact geology and some post-impact layering.

Key words: Pelarda Formation, Iberian System, Upper Eocene/Oligocene, Azuara impact structure, proximal impact ejecta, pyroclastic flow

1 Associate Geological Museum Barcelona (Spain); fclaudin@xtec.cat
2 University of Würzburg (Germany), Faculty of Philosophy; kernstson@ernstson.de
3 Formerly DEMINEX oil company; retired geologist; wolfgang.monninger@t-online.de

Content

1	Introduction	3
2	Previous studies - overview	7
2.1	Lithology	7
2.2	Source for the Pelarda Fm. material	8
2.3	Age of the Pelarda Fm. deposit	9
3	Previous studies - geological setting, layering, and petrographic features	9
3.1	Geological setting	9
3.2	Layering	16
3.3	Petrographic features	16
	<i>Shock metamorphism</i>	16
	<i>Mesosopic deformations</i>	19
	<i>Impact spallation</i>	21
4	New investigations	22
4.1	Methodology	23
4.2	Investigated locations	23
4.2.1	Salcedillo S1	24
4.2.2	Salcedillo S 2	37
4.2.3	Road from Olalla to Fonfría (S 3 and S 4 in Fig. 6 and Fig. 23)	38
4.2.4	Contacts	42
4.3.	Granulometric and textural analyses	48
4.4	Petrographic analyses of thin sections	49
	<i>Shock metamorphism (shock effects)</i>	49
4.5	Paleocurrent analysis	52
4.6	Sedimentary environment	52
4.7	Origin of the clasts	54
4.8	Age	54
4.9	More Pelarda Fm. ejecta deposits: the San Roque deposit	55
5	Discussion	55
6	Conclusions	58
	References	59
	Appendix I: The Azuara impact cratering process and ejecta formation in eight images - schematic	67
	Appendix II: The Ermita de San Roque Pelarda Fm. ejecta deposit	71

1 Introduction

The Pelarda Formation (Fig. 1) covers an area of about 12 x 2.5 km² (Fig. 2), has a thickness of in part up to 400 m, and is exposed between 1,100 and 1,450 m altitude in the highest parts of a mountain chain within the Alpidic Iberian system (Fig. 3). First described by Monninger (1973) and Carls & Monninger (1974), the origin of the Formation experienced various and quite different explanations like fluvial (Carls & Monninger 1974; Adrover et al. 1982; J. Smit 2000 (written communication), alluvial fan (Lendínez et al. 1989, Pérez 1989; Aurell et al. 1993; Aurell 1994; Cortés et al. 2002; Díaz-Martínez et al. 2002 a, b, c; Díaz-Martínez 2005) and meteorite impact (Ernstson & Claudin 1990, Ernstson & Fiebag 1992, Rampino et al. 1997 a, b; Claudin et al. 2001; Ernstson et al. 2002, 2003; Claudin & Ernstson 2003; Ernstson 2004) deposition.

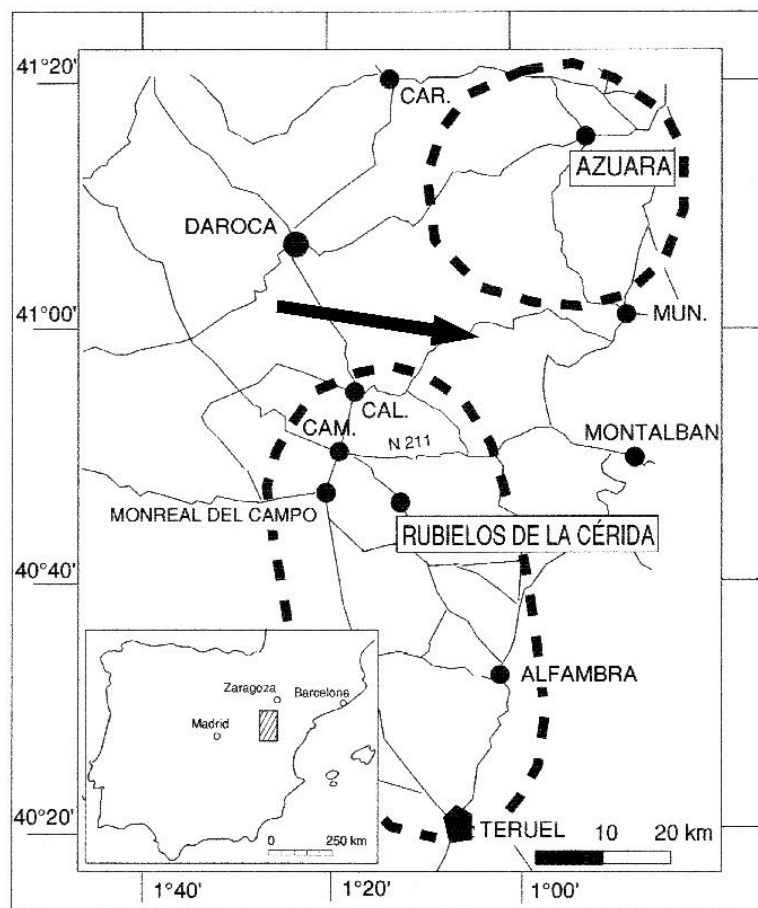


Fig. 1. Location map for the Azuara and Rubielos de la Cérída impact structures in Spain. Modified from Ernstson et al. (2002). The arrow focuses on the occurrence of the Pelarda Fm. in detail outlined in Fig. 2. CAM = Caminreal, CAL = Calamocha, CAR = Cariñena, MUN = Muniesa.

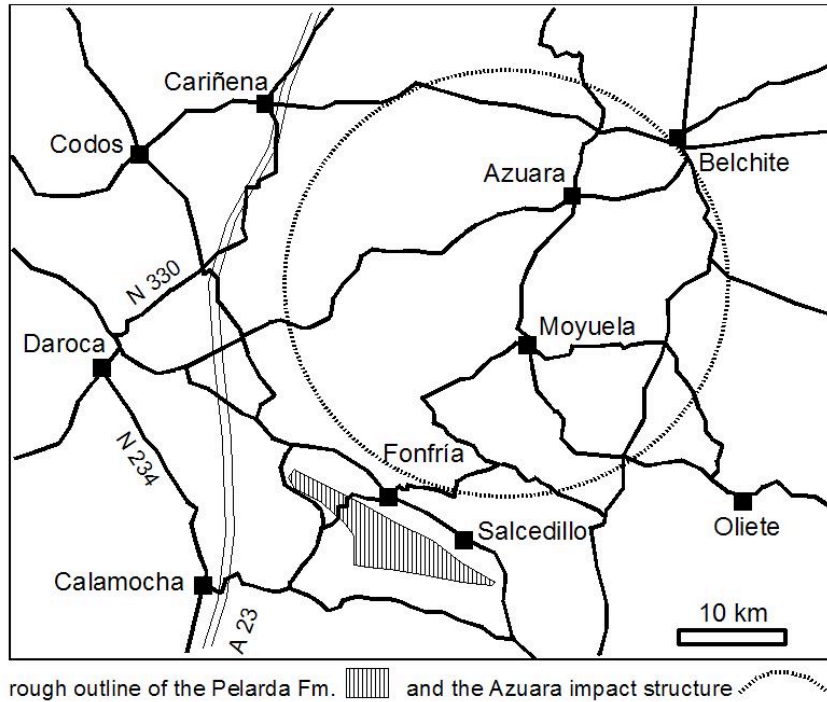


Fig. 2. Location map for the Pelarda Fm.



Fig. 3. View of the densely forested Pelarda Formation deposit forming the highest mountains (Retuerta 1,512 m) of the Sierra de la Pelarda (or Sierra de Fonfria).

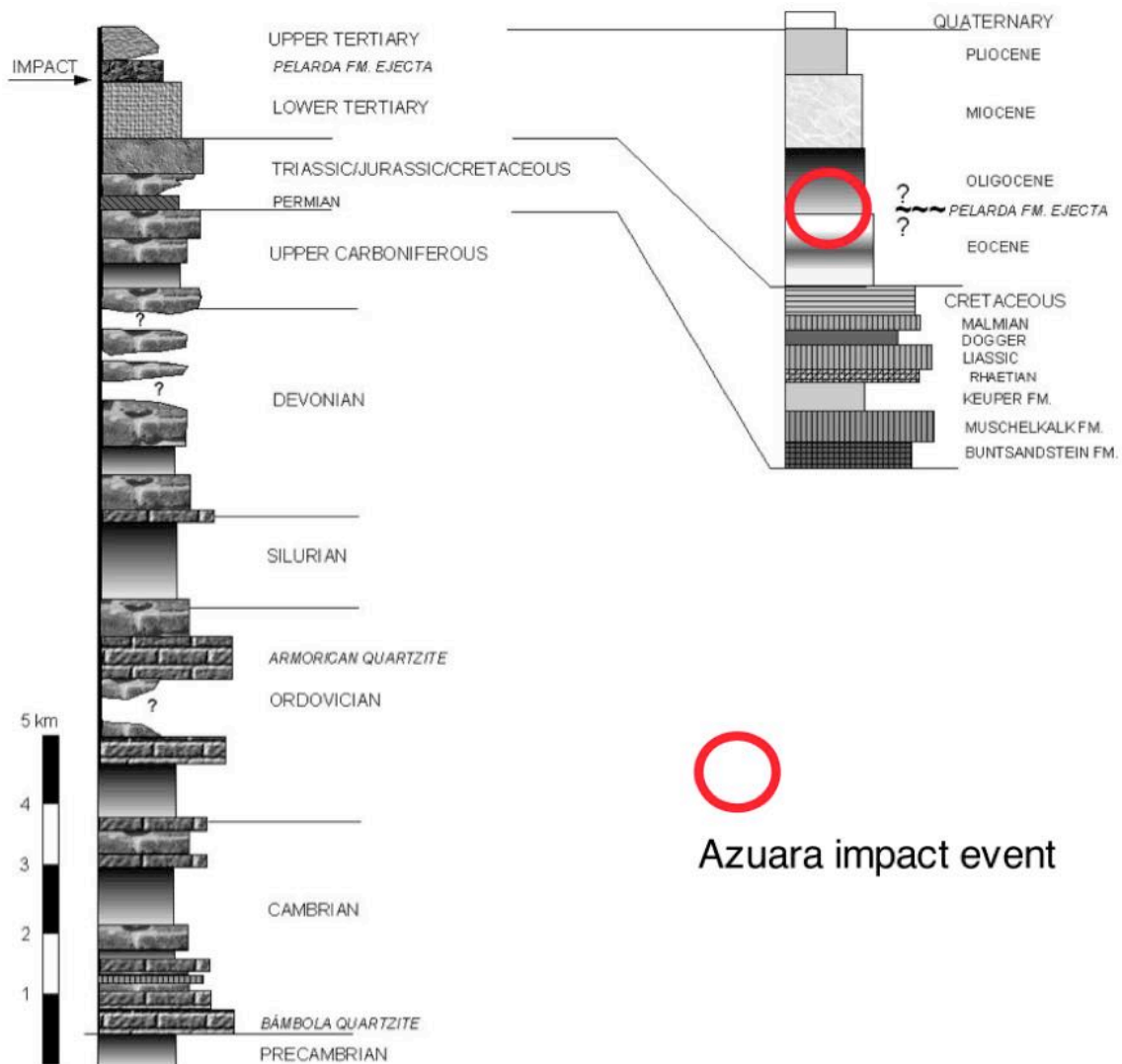


Fig. 4. The Pelarda Fm. and the Azulara impact event within the stratigraphy of the Iberian Chain. Data from Carls & Monninger (1974) and ITGE (1991). Modified from Ernstson et al. (2002).

The meteorite impact model considers the Pelarda Fm. to be ejecta of the about 40 km-diameter Azulara impact structure located at the margin between the Iberian Chain and the Ebro Basin in northeast Spain (Fig. 1). In Fig. 1, the Azulara structure is sketched as part of the proposed multiple-impact scenario also comprising the Rubielos de la Cérída elongated impact basin (Ernstson 2001a, b, 2002, 2003; Hradil et al. 2001, Claudin et al. 2001). Stratigraphically, the Pelarda Fm. and the impact event are positioned in the column of Fig. 4.

The Azulara structure first described as a probable impact crater by Ernstson et al. (1985) has undergone a long and curious history. In the 1985 paper, Ernstson et al. presented clear and unambiguous shock effects in Azulara rocks like planar deformation features (PDFs) in quartz, as well as other typical impact-related features. Consequently, Azulara became listed as a confirmed impact structure (Grieve & Shoemaker 1994, Hodge 2010, Norton

2002) and was included in the Earth Impact Database of established impact structures conducted by the Canadian Geological Survey (R.A.F. Grieve and co-workers). Later, more evidence for the impact nature of Azuara in the form of additional shock effects (e.g., shock melt, diaplectic glass, shatter cones), abundant monomictic and polymictic breccias, extensive megabreccias, dislocated megablocks, and geophysical anomalies was presented (Ernstson et al. 1987, Fiebag 1988, Ernstson 1994, Ernstson & Fiebag 1992, Ernstson et al. 2001, Ernstson et al. 2002). In 1990, the Pelarda Fm. was for the first time suggested to be Azuara proximal impact ejecta (Ernstson & Claudin 1990) thus also supporting the extraterrestrial origin of the crater. The impact nature of the Pelarda Fm. was mainly attributed to the abundant occurrence of shock-metamorphic effects (multiple sets of planar deformation features, PDFs, and multiple sets of planar fractures, PFs, in quartz) as well as on high-pressure/short-term deformations (e.g., rotated fractures) of clasts regularly found in the deposit (Ernstson & Claudin 1990).

Surprisingly, in 2003 when the management of the Canadian impact database had changed from the Geological Survey to the university of New Brunswick (J. Whitehead and J. Spray), Azuara was removed from that database despite all established impact evidence the clear and unambiguous shock-metamorphic effects included. For insiders, the reason for the removal of the Azuara impact structure is obvious (Ernstson & Claudin 2013b). However, this will not be discussed here, but playing a certain role in the discussion about the Pelarda Fm., the fact of the removal is worth mentioning here.

As proximal impact ejecta, the Pelarda Fm. attracts considerable attention, because ejecta deposits of such a size and extension are extremely rare among terrestrial impact structures. The reason for the poor preservation of this special kind of sediments is the in general rapid erosion of the ejecta deposits even in the case of large craters. It has been suggested that diamictites commonly interpreted as glacial (tillite) deposits are in fact preserved impact ejecta of unidentified impact structures (Oberbeck et al. 1993, Rampino et al. 1992, 1994, 2017), however no respective studies in proof of this model have been published so far (also see Reimold et al. 1997).

Apart from the many distal occurrences (e.g., Addison et al. 2005), Haines 2005, Glikson 2005, Hassler et al. 2011, Glikson et al. 2016, Glikson & Pirajno 2018) numerous ejecta deposits from various established impact structures have carefully been studied (e.g., Ries [Hüttner 1969, Hörz 1982], Chesapeake Bay [Horton et al. 2005, Horton & Izett 2006]), Chicxulub [Pope et al. 1999, 2005, Schulte & Kontny 2005, and others], Haughton [Osinski et al. 2005]), the generation of ejecta deposits is still poorly understood (e.g., Housen & Holsapple 2011, Osinski 2007, Osinski et al. 2011, 2013). While a ballistic sedimentation and emplacement of impact ejecta on airless bodies is general accepted (Oberbeck 1975), new models suggesting surface flow similar to pyroclastic flow or as impact melt-rich ground-hugging flow (e.g., Newsom et al. 1986, Osinski et al. 2004, Artemieva 2006, Meyer et al. 2008, 2011, Artemieva

et al. 2013, Stöffler et al. 2013, Siegert et al. 2017) in addition to ballistic emplacement are also taken into consideration.

This new and increased interest in impact ejecta and ejection processes initiated a new and comprehensive study of the Pelarda Fm. within the last years including new separate companion deposits the results of which are presented here.

A more comprehensive paper on the Pelarda Fm., in particular focusing on new geologic mapping results and showing a host of outcrop and sample photos and stratigraphical columns, has recently been published in Spanish language (Claudin & Ernstson 2018).

2 Previous studies - overview

2.1 Lithology

In Fig. 5, a typical aspect of a Pelarda Fm. outcrop is shown, although the facies may change considerably as is in detail described below.

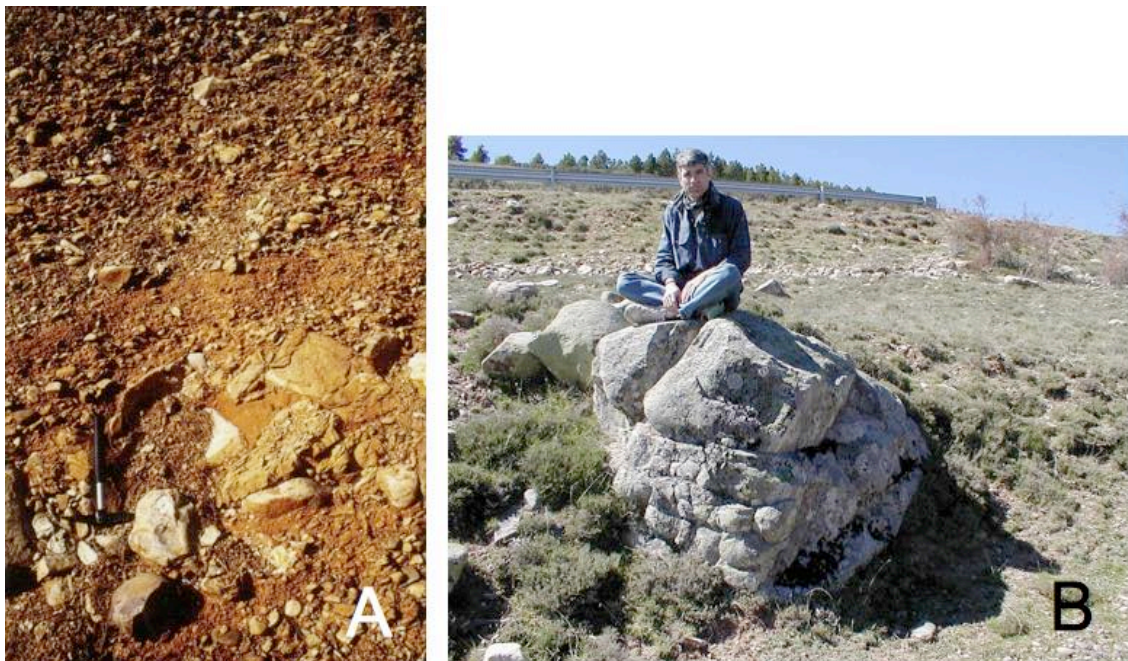


Fig. 5. A: Typical aspect of the Pelarda Fm. facies that, however, may change considerably throughout the deposit. B: Large quartzite clast from the Pelarda Fm.

Lithologically, the Pelarda Fm. has been described as -- a boulder conglomerate composed of mostly well-rounded clasts (predominantly Paleozoic sediments) in an unconsolidated gravelly yellowish-brownish matrix (Carls & Monninger 1974),

- a diamictite with conglomeratic intercalations in a sandy-silty-clayey matrix (Ernstson & Claudin 1990, 2002), and
- conglomerates and diamictites composed of rounded to subrounded quartzite clasts eroded from the local basement and immersed in a sandy-silty-clayey matrix apparently without any orientation and configuration (Cortés et al. 2002; Díaz-Martínez et al. 2002 a; Díaz-Martínez 2005).

In all cases, the practical lack of or at most very poor stratification and the distinctly bad sorting including quartzite clasts up to the size of 1 m (Díaz-Martínez 2005) or even much larger (Fig. 5) have been pointed out (Ernstson & Claudin 1990, 2002).

2.2 Source for the Pelarda Fm. material

As for its origin, the Pelarda Fm. deposit has as listed above been attributed to fluvial processes, alluvial processes and meteorite impact processes (impact ejecta).

For the models of fluvial and alluvial deposition, the source of the material has been located in the NW (Carls & Monninger 1994) and in the S-SE, respectively (Cortés et al. 2002; Díaz-Martínez et al. 2002 a, b, c; Díaz-Martínez 2005), while the impact emplacement model considers a source in the NE (Ernstson & Claudin 1990, 2002; Ernstson & Fiebag 1992). The S-SE direction suggested by Díaz-Martínez et al. (2002 a, b, c) and Díaz-Martínez (2005) lacks any support by specific investigations, e.g., by paleocurrent studies. Carls & Monninger (1974) deduce the NW source location from the many Bámbola quartzite clasts that contribute to the Pelarda Fm. and are assumed to originate from the outcropping Paleozoic Bámbola layers near Codos village (see Fig. 2). Cortés et al. (2002) believe that the material of the Pelarda Fm. is a proximal alluvial deposit, which developed at the base of a hypothetical massif produced by faulting during the Upper Miocene - Pleistocene (a faulting that is said to have affected the Calatayud- Montalbán basin). Moreover, according to Cortés et al. (2002) the Paleozoic rocks in the region under discussion never attained significant altitudes until the Miocene.

In the impact ejecta model of Ernstson & Claudin (1990), the Pelarda Fm. material is derived from NE corresponding to the center of the Azuara structure. The authors assume that the impact affected a target composed to a considerable amount (up to 2,000 m thickness or more) of Tertiary molasse sediments from the Alpidic Iberian System. Ernstson & Claudin (1990) analyzed more than 400 sets of striations on the surfaces of clasts embedded in the Pelarda Fm. resulting in a clear NE strike accumulation. The striae are suggested to have been formed in the latest phase of ejecta emplacement and thus to have preserved the main direction of the ejecta trajectory (also see below).

The early petrographic description by Carls & Monninger (1974) noted the evident complete lack of limestone clasts in the deposits, which was paleogeographically related with the source for the Pelarda Fm. material. Meanwhile, we were able to verify the occurrence of Jurassic and/or Cretaceous limestone cobbles and boulders, although in fact represented scarcely, which will in more detail be discussed later. In the course of our field work we were also able to establish the existence of coherent Buntsandstein megaclast (up to the size of 9 m) embedded in the Pelarda Fm. material otherwise not mentioned in the literature. Opponents of the impact model (Cortés et al. 2002; Díaz-Martínez et al. 2002 a; Díaz-Martínez 2005) consider the megaclasts to be thin sandstone layers belonging to the (from their point of view) alluvial fan stratigraphy.

2.3 Age of the Pelarda Fm. deposit

The ages so far proposed for the deposition of the Pelarda Fm. material are the Paleogene (Carls & Monninger 1974; Adrover et al. 1982; Ernstson & Claudin 1990; Ernstson & Fiebag 1992; Ernstson et al. 2002; Ernstson et al. 2003; Claudin & Ernstson 2003), the Miocene (IGME 1981) and the Quaternary (ITGE 1989; ITGE 1991; Aurell et al. 1993; Aurell 1994; Smit 2000 (written comm.); Cortés et al. 2002; Díaz-Martínez et al. 2002 a, b, c; Díaz-Martínez 2005). Among these authors, Cortés et al. (2000), Díaz-Martínez et al. (2002 a, b, c) and Díaz-Martínez (2005) suggest a Pliocene or Pleistocene age and consider the Pelarda Fm. an alluvial fan deposit (of the “raña” type) that accumulated at the base of a former Paleozoic relief meantime fallen to denudation and today no longer existent. Nevertheless, at the same time, they strangely enough consider the deposit as being still under investigation and admit a Paleogene age as proposed by Adrover (1982).

3 Previous studies - geological setting, layering, and petrographic features

3.1 Geological setting

As noted in their paper, Ernstson & Claudin (1990) appreciated the early sound geologic field work on the Pelarda Fm. by Carls and Monninger (1974) and conceded that new outcrops and especially petrographic work had enabled the development of the new impact model. Both the early work spanning the geologic frame and the hitherto existing petrographic data are summarized in the following.

The Pelarda Fm. is located between the Azuara structure and the Rubielos de la Cérda impact basin and extends more or less tangentially with respect to both (Fig. 1, Fig. 2). According to the existing geological mapping

(ITGE 1991; ITGE 1989; IGME 1977/81) and to own field data, Paleozoic, Mesozoic, Eocene to Lower Oligocene, Lower to Middle Miocene, and Quaternary rocks make the contact (Fig. 6), although in the official IGME (1977/81) and ITGE (1989, 1991) maps the Pelarda Fm. does not exist and is instead mapped as Miocene not further itemized (IGME), and Quaternary (ITGE). More inconsistencies between our own field work and the existing official maps will not be considered here unless they are immediately related with the matter under discussion.

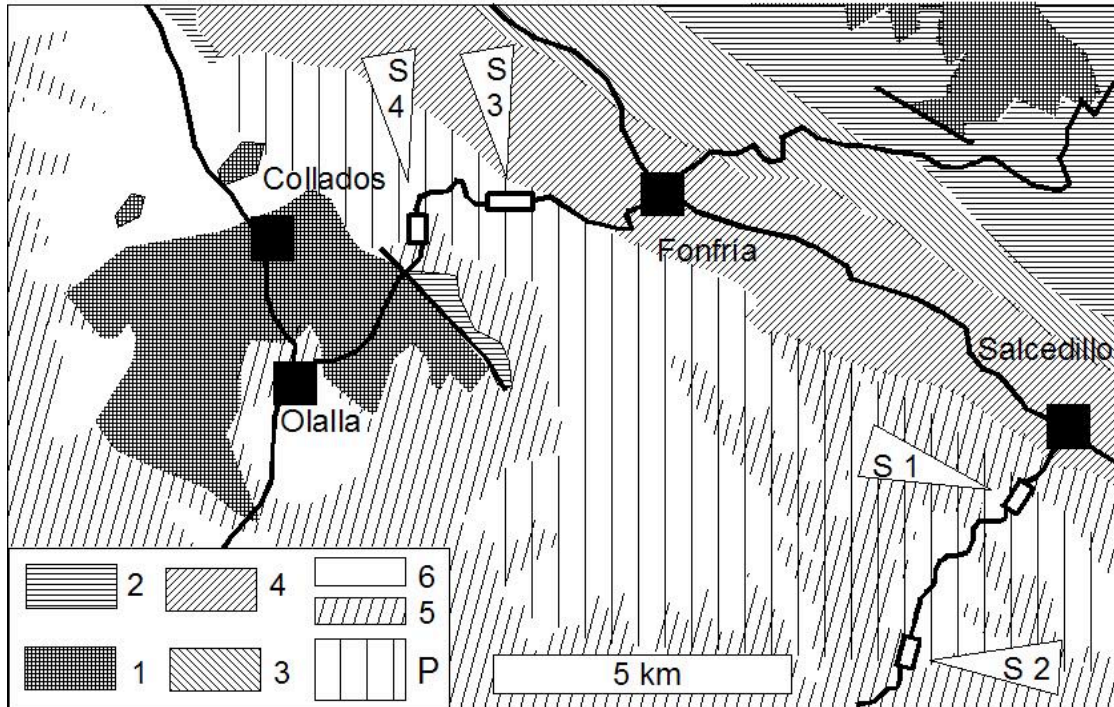


Fig. 6. Geological general map for the region of the Pelarda Fm. 1 = Paleozoic, 2 = Triassic, (?) Jurassic, 3 = Cretaceous, 4 = Eocene-Lower Oligocene, 5 = Miocene, 6 = Quaternary, P = Pelarda Fm. S1 - S4 = outcrop locations examined in the new field campaigns. S1 is preferentially addressed in this paper.

Paleozoic contact zone

The kilometer-sized Paleozoic complexes are exposed near Olalla and Collados (Fig. 6, 7), constituting there the "footwall" of the Pelarda Fm. According to Monninger (1973) and ITGE (1991), the Embid, Jiloca, Ribota, Huérmeda, Daroca, Valdemedes, Murero and Almunia Formations contribute to the stratigraphy, where lithologically slates, sandstones, dolomites, limestones, quartzites and calcareous siltstones dominate. Especially the rocks of the Valdemedes and Murero Fms. are heavily fractured through and through exhibiting grit brecciation and mortar texture. Here, Monninger (1974) mapped extensive bands of "mylonites" (his designation; Fig. 8) striking 130°.



Fig. 7. The contact between the Pelarda F. and the Paleozoic unit is rather diffuse, because the Quaternary debris from weathering of the Pelarda layers are moving downhill.



Fig. 8. Monomictic movement breccias ("mylonites", Monninger [1973]) - Paleozoic near the contact to the Pelarda Fm. These "monomictic movement breccias" also refer to strongest earthquakes and massive landslides of a strength and character that have not been described for Alpine movements in the region (and also elsewhere).

These "mylonites" (we prefer the term *monomictic movement breccias* (see the discussion by Reiff [1978]) together with abundant breccia dikes and a suevitic breccia (Fig. 9) adjacent to the Pelarda Fm. outcrops near Olalla (UTM coordinates 0656513 E/4539035 N) are now interpreted as originating from the proposed Azuara/Rubielos de la Cérda impact event and are in more detail described and discussed in Ernstson et al. (2002) and Claudin & Ernstson (2012).



Fig. 9. From the Paleozoic - Pelarda Fm. contact zone: Sawed and polished surface of a polymictic suevite breccia exhibiting flow and breccia-within-breccia texture. Coin diameter 18 mm.

Mesozoic contact zone

The Mesozoic of the contact is represented by Muschelkalk, Keuper and (?)Jurassic rocks). Like the Paleozoic rocks, the Mesozoic rocks are intensively fractured and heavily brecciated (Fig. 10). The Muschelkalk limestones and dolomites partly overlain by the upper part of the Pelarda Fm. are abundantly exhibiting mortar texture and hosting impact breccia dikes (Ernstson et al. 2002). Among these breccia dikes, accretionary lapilli have been established to contribute to the dike material and in a few cases to make the breccia matrix in form of lapillistone (Fig. 11). Quartz grains, limestone fragments, fragments of

Paleozoic metamorphic rocks and accretionary grains can form the nucleus of the lapilli.



Fig. 10. Large volumes of pervasively crushed Muschelkalk limestones near the contact to the Pelarda Fm.

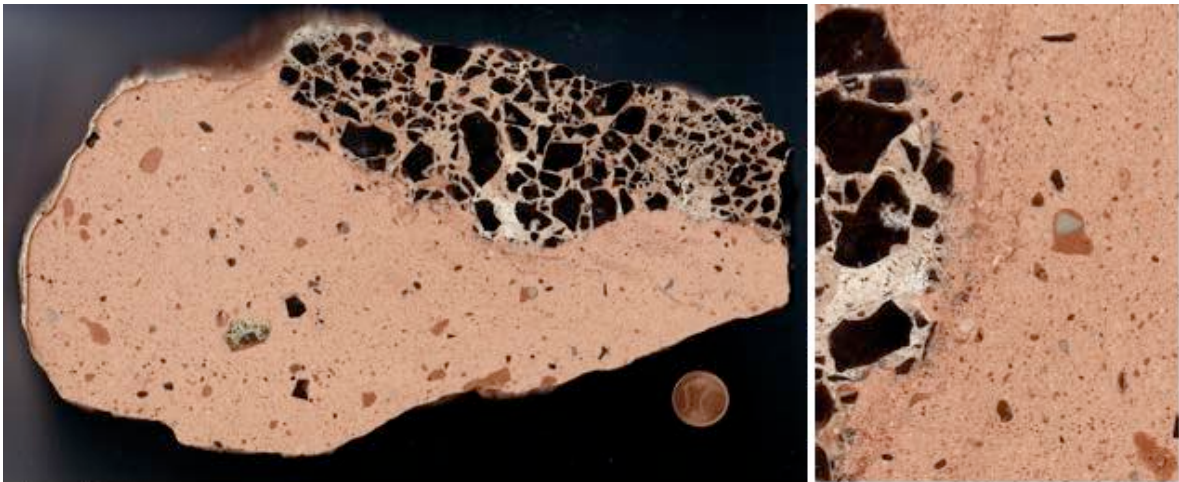


Fig. 11. From the Muschelkalk - Pelarda Fm. contact zone: Dike breccia composed of Muschelkalk fragments (dark; coin diameter 16 mm) in accretionary lapilli matrix (lapillistone; detail to the right). The lapillistone occurrence will be addressed also later.

The contact between the Pelarda Fm. and the Paleozoic/Mesozoic (see 4.2.4 Contacts; Fig. 52) is in part masked by an extensive deposit of an unconsolidated breccia composed of angular, exclusively Paleozoic clasts. The

portion of a shaly-sandy matrix of reddish-brownish color is poor. The breccia has already been mapped and described ("rim breccia") by Monninger (1973) who conceded that origin and age of the deposit were problematic. From the comparison with dislocated (allochthonous) megablocks exposed in the Azuara impact structure and in part exhibiting a very similar facies (Ernstson & Fiebag 1992), an origin from impact excavation, ejection and emplacement must be considered. The immediate contact with the Pelarda Fm. and the basal breccia (suevite breccia; see Fig. 5) obviously overlying the rim breccia substantiates this interpretation. In the official geological maps (ITGE, IGME) the rim breccia is attributed to the Miocene. The rim breccia is in more detail discussed in 4.2.4,

Lower Tertiary contact zone

Conglomerates, claystones, sandstones, siltstones and levels of conglomerates, red clays, charophyte limestones and marls are represented in the Upper Eocene - Lower Oligocene stratigraphy. Near Fonfría (Fig. 12), beds of conglomerates of the Eocene-Oligocene are exposed immediately below the base of the Pelarda Fm., and, without exception, the limestone pebbles and cobbles exhibit peculiar surface deformations in the form of striations, polish and remarkable imprints (Fig. 13). It is suggested that the plastic deformations within the conglomerates have originated from the highly energetic emplacement of the landing Pelarda Fm. ejecta.



Fig. 12. Lower Eocene-Oligocene conglomerates near the contact to the base of the Pelarda Fm. ejecta.



Fig. 13. From the Eocene/Oligocene - Pelarda Fm. contact zone: limestone cobbles from a conglomeratic bed with imprints, heavy striations and polish all around.

In the zone of Salcedillo (Fig. 6) the conglomeratic levels are polygenetic, occur as lenticular bodies with thicknesses not exceeding 1.5 m, and are intercalated within sandy layers. No plastic deformations of the components like those in the Fonfría conglomerates can be observed here.

Upper Tertiary contact zone

According to ITGE (1991) and own field work, the Lower to Middle Miocene is built up of red clays, sands and conglomerates. In the environs of Olalla, the Miocene conglomerates as mapped in the existing cartography (ITGE 1991) prove in many cases to be in fact breccias. These breccias are polygenetic, heterometric and matrix-supported. They form transversally oriented lenticular

bodies displaying variable but in general small lateral extension (less than 5 m). Longitudinally, the breccia bodies are drop-to-tongue-shaped and elongated in the direction of dip being some 30-35° towards SW. The age of the breccias is left to assumptions.

Quaternary

The Quaternary is composed basically of material derived from weathering and erosion of the Pelarda Fm. The contact to the underlying stratigraphical units is always discordant implying more or less zero dip of the Quaternary.

3.2 Layering

According to the early general field work of Ernstson & Claudin (1990), the Pelarda Fm. deposit shows a very rough stratification into three parts. The contacts between the lower, middle and upper zones prove to be gradual and not anywhere near traceable. On the whole, the zones differ by clast lithology, clast size and shape, and matrix composition. A matrix-supported texture is largely to be observed. Only locally developed bedding planes enabled the measurement of strike and dip with a southwest and northeast dip preference (also see below and Fig. 21).

3.3 Petrographic features

Shock metamorphism

The petrographic work on the Pelarda Fm. has in the past concentrated on shock-metamorphic microscopic deformations and on mesoscopic deformations of clasts. Pelarda Fm. shock effects in the form of multiple sets of planar deformation features (PDFs; Figs. 14, 15), multiple sets of planar fractures (PFs, Fig. 17), mosaicism and kink bands in quartz have been reported in Ernstson & Claudin (1990), Ernstson & Fiebag (1992), Ernstson et al. (2002) and Claudin & Ernstson (2003). The shock-metamorphic PDFs in Armorican and Bámbole quartzites from the Pelarda Fm. were unambiguously confirmed in analyses performed by Guerrero (2000) and Therriault (2000) (Fig. 16).

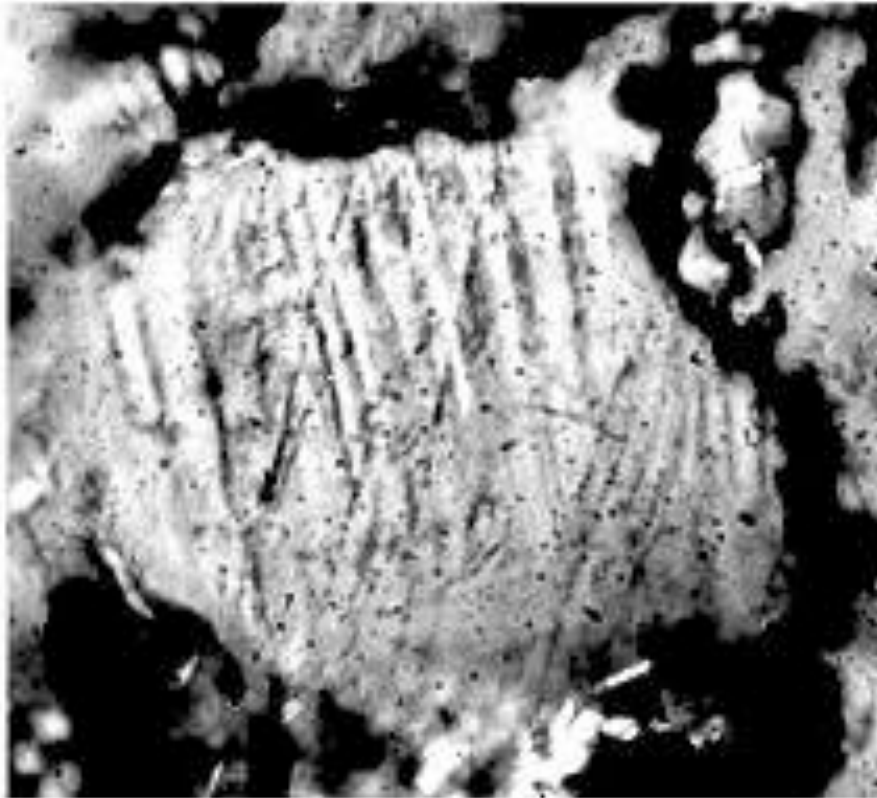


Fig. 14. Decorated planar deformation features (PDFs) in quartz from the Pelarda Fm. Photomicrograph, crossed nicols. The crystallographical orientations of the sets are {10-13} and {10-12}. The field is 200 μm wide. Analysis and image: Guerrero (2000).

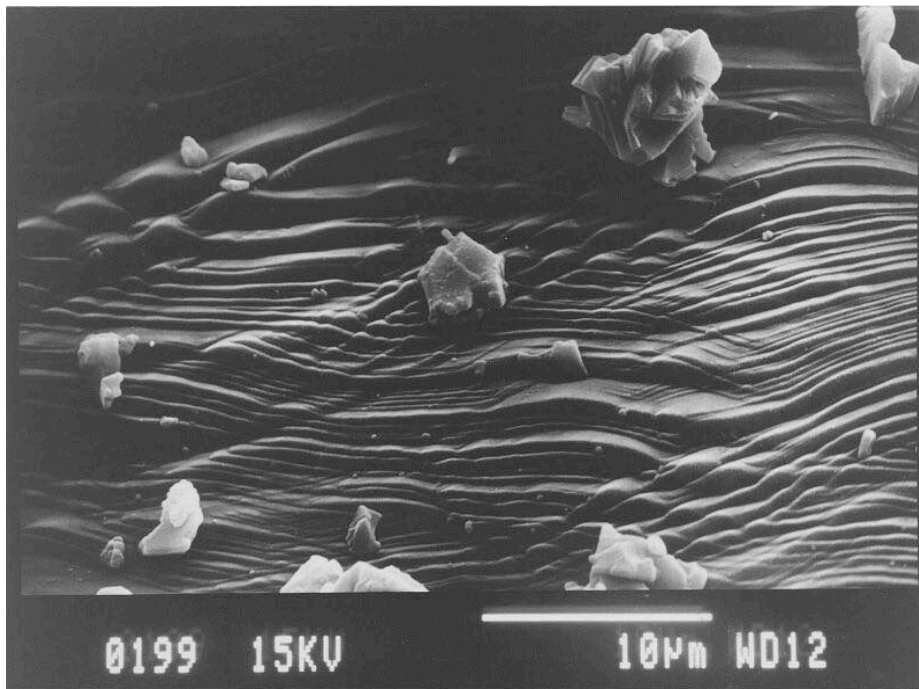


Fig. 15. SEM image of two sets of crossing PDFs in quartz; shocked Bámbola quartzite clast from the Pelarda Fm.

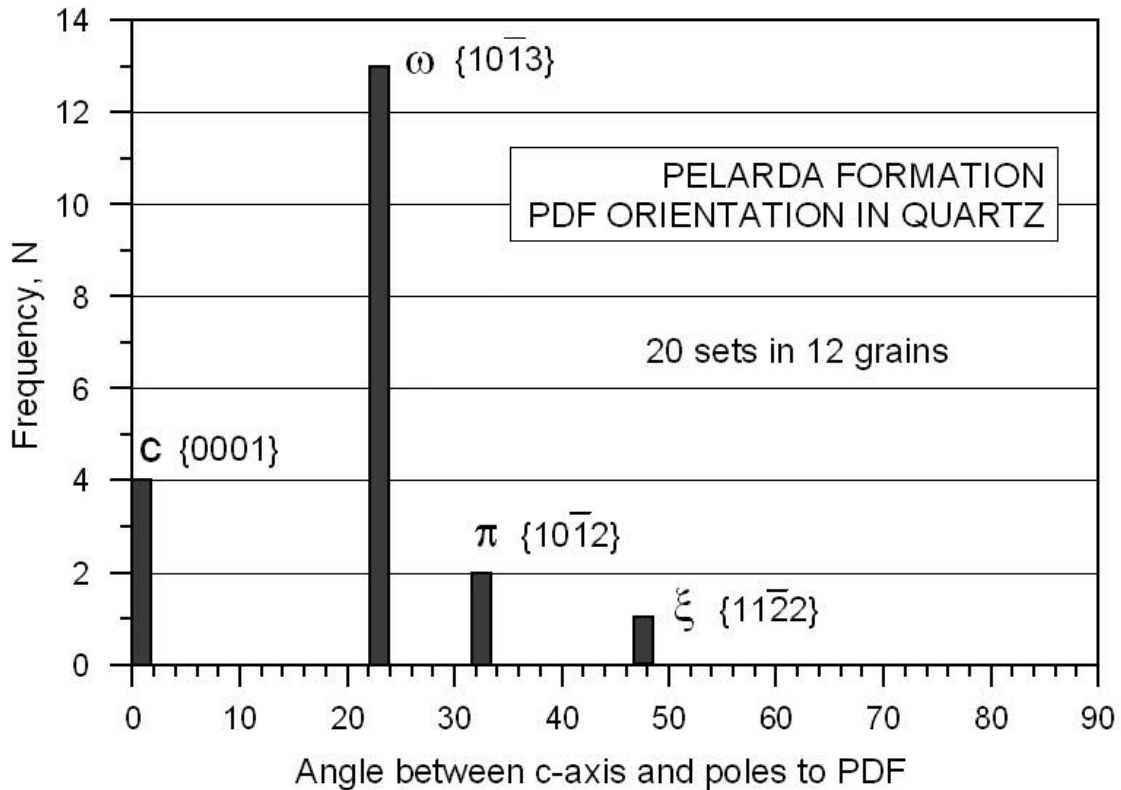


Fig. 16. Frequency diagram of crystallographic orientation of planar deformation features (PDFs) in quartz from the Pelarda Fm. Data from Therriault (2000).

In Fig. 16, a frequency diagram of crystallographic orientation of PDFs from Pelarda Fm. rocks is shown. The prevailing ω and, subordinately, π planes suggest shock pressures exceeding 10 GPa (= 100 kbar) (Stöffler & Langenhorst 1994, Grieve et al. 1996). Other parameters such as PDF density, sharpness, spacing, and spreading over the grain were additionally analyzed (Therriault 2000): Up to three sets of PDFs per grain were found in the Pelarda Fm. quartz grains. 87.5 % of all sets exhibit a PDF spacing < 1 μm , 12.5 % between 1 - 5 μm . The spreading over the grain is in most cases 100%, and the PDF density always high. Practically all sets are decorated. All shocked grains have reduced birefringence of 0,004 - 0,008. The prevailing {10-13}, ω , and {10-12}, π , PDF orientations in the shocked samples from the Azuara structure are unusual considering the sedimentary (porous) target in which {11-22}, ξ , and {10-11}, r,z, directions commonly are more typical (Stöffler et al. 1994, Grieve et al. 1996). The "crystalline" signature of the Azuara PDFs, however, may be explained by the lithology of the dense shock-affected quartzite clasts. Cortés et al. (2002), Díaz-Martínez et al. (2002) and Díaz-Martínez (2005) basically denying any impact evidence don't take the shock effects as being existent.



Fig. 17. Multiple sets of planar fractures (PFs) in quartz. Bámbola quartzite cobble, Perlarda Fm.

Mesoscopic deformations

Mesoscopic impact evidence in the Pelarda Fm. deposits is revealed by the abundant occurrence of heavily deformed cobbles and boulders exhibiting striations (Fig. 18, 19) and polish even on the surfaces of quartzite clasts, rotated fractures and irregular fractures with complex bifurcations (Fig. 20).



Fig. 18. Pelarda formation: large striated quartzite boulders. – Science may yield curiosities: When the impact ejecta origin for the Pelarda formation had been suggested and an article (Ernstson & Claudin 1990) was printed showing exactly this photo of the heavily striated quartzite boulders, these heavyweight objects resting near a drop-off had disappeared only shortly after and were never seen again.



Fig. 19. Multiple sets of striae on quartzite cobbles from the Pelarda Fm. The field is 2.5 cm wide.



Fig. 20. Heavily deformed however coherent Armorican quartzite boulders from the Pelarda Fm.

Being embedded in a soft, unconsolidated matrix, these deformations of coherent cobbles and boulders are in proof of high confining pressure and short-term deformation upon applied stress compatible with highly energetic excavation, ejection and emplacement processes in the various stages of impact cratering (Melosh 1989). As has been suggested earlier (Ernstson & Claudin 1990), the Pelarda Fm. ejecta emplacement is reflected by a preferential orientation of striae pointing to the center of the Azuara impact structure (Fig. 21).

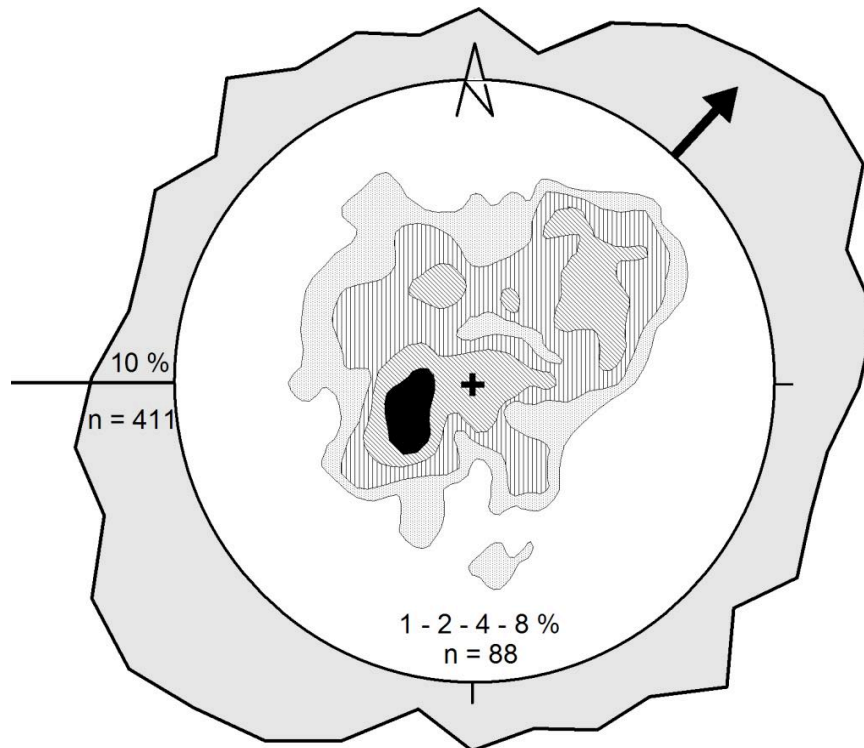


Fig. 21. Pelarda Formation: Equal area plot of the normals to locally developed bedding planes and rose diagram of striae azimuth. Note the correlation of both distributions. The arrow points to the center of the Azuara impact structure. Modified from Ernstson & Claudin (1990).

Opponents of an impact scenario and advocates of an alluvial fan deposition (Cortés et al. 2002; Díaz-Martínez et al. 2002 a, Díaz-Martínez 2005) explain the peculiar *in situ* deformations by tectonic forces thus requiring an important local tectonic phase in the Quaternary otherwise nowhere evident, however. Moreover with regard to the soft unconsolidated matrix, the heavily broken however coherent cobbles like those shown in Fig. 20 cannot possibly be explained fracture-mechanically by tectonics.

Impact spallation

Abundantly, quartzite boulders show a typical fracturing that can be ascribed to shock spallation. Spallation is a well-known process in fracture mechanics as well

as in impact cratering and has been investigated theoretically and experimentally by many researchers. Unfortunately, it is less well known that spallation can also be observed in nature as an actually existing geologic phenomenon in and around impact structures. Spallation takes place when a compressive shock pulse impinges on a free surface or boundary of material with reduced impedance (= the product of density and sound velocity) where it is reflected as a rarefaction pulse. The reflected tensile stresses lead to detachment of a spall or series of spalls. Prominent spallation effects have been reported for shocked Buntsandstein conglomerates exposed around the Azuara/Rubielos de la Cérica impact structures. Details about these geologic spallation features have been described in Ernstson et al. (2001) and Ernstson (2014). In impact research, spallation, which as a shock effect can be observed down to microscopic scale in shocked quartz grains, is largely ignored, and also in recent relevant literature (e.g. French and Koeberl 2010) spallation as an important shock indicator is not even mentioned.



Fig. 22. The peculiar concave fracture of a quartzite boulder in the field of the Pelarda formation deposit is explained by dynamic shock spallation. Typically and for geometrical reasons, the concave fracture plane mirrors the original convex boulder surface (as shown dashed in the left photo). This typical shock spallation effect is abundantly observed in the field of the Pelarda formation ejecta.

4 New investigations

Now as before, the outcrop conditions in the large forest area corresponding with the Pelarda Fm. deposit are poor. Although a ramified road network exists enabling easy access, the roads are only sporadically carving the ground, and Quaternary debris are broadly curtaining the original layering and stratigraphy. Therefore in the past, the sidewalls of the road between Fonfría and Olalla more or less traversing the Pelarda Fm. deposit (Fig. 6) gave the most instructive insight. The new investigations are mainly based on a further opportunity to study the Pelarda Fm. in more detail in sections along a cartway starting in the village of Salcedillo and also traversing the deposit more or less perpendicularly (Fig. 6).

4.1 Methodology

The present new study of the Pelarda Fm. is based on the following methodological proceeding:

- re-examination of the hitherto existing field data
- realization of stratigraphical columns as far as enabled by the outcrop conditions, and possible correlations,
- sampling and analysis of more than 150 clasts from the diamictic levels; measurement of roundness and sphericity according to the visual criteria of Powers (1953) and Krumbein & Sloss (1955),
- petrographic characterization as well as analysis of 35 thin sections of the collected rudites,
- sampling and petrographic analysis including 25 thin sections of sandstones intercalated between the diamictic levels as well as from isolated levels,
- analyses of the sedimentary structures and identified facies,
- analysis of paleocurrents as far as permitted by the outcrop conditions, and
- sampling of fossils from accessible levels for dating purposes.

4.2 Investigated locations

In the following we consider four locations of differing importance. They are designated and marked as S1, S2, S3 and S4 in the map of Fig. 6, and their general stratigraphic position is shown in Fig. 23. The Salcedillo location no. S1, because of its extension and the possibility to study the contacts between different units, has supplied the crucial host of new data enabling the construction of stratigraphic columns (Claudin & Ernstson 2018). S2, separated from S1 by a long section of the cartway without exposures (Fig. 23), supplies some insight into the upper part of the Pelarda Fm. S3, covering the lower and middle part along the road from Fonfría to Olalla (Figs. 6, 23), serves for comparison with the Salcedillo outcrops. S4 eventually also sheds some light on the layering conditions in the upper part of the Pelarda Fm.

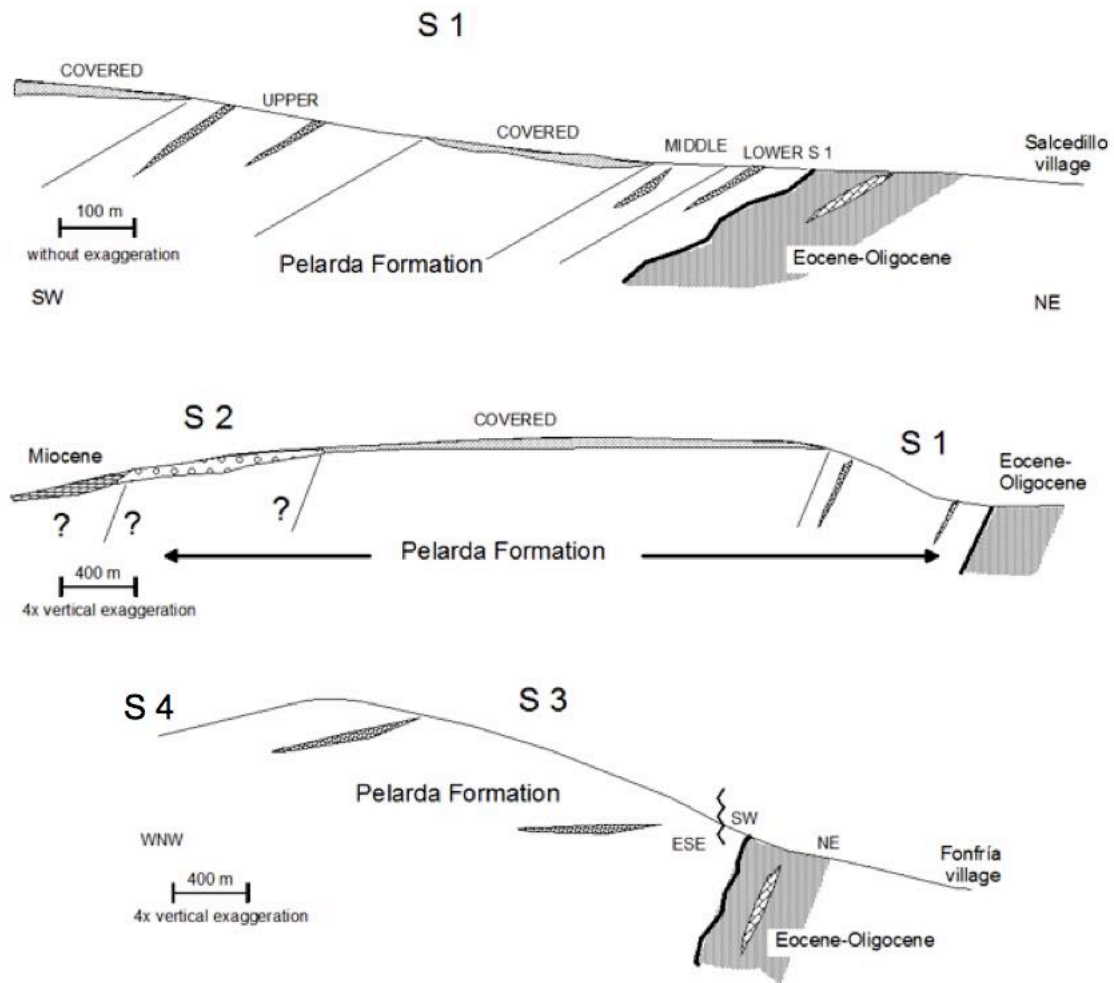


Fig. 23. The investigated locations in their general stratigraphic position. For details see the following text.

4.2.1 Salcedillo S1

The outcrop S1 of the Salcedillo zone, easily accessible along the way from Salcedillo village in a SW direction, has been divided into three parts, Salcedillo Lower, Middle, and Upper S1. Middle S1 and Upper S1 are separated by a segment lacking any significant outcrops (see Fig. 23).

Salcedillo Lower S 1

Lower S1 starts at UTM 30667751 E / 4536032 N (c. 1200m altitude) with a first series of rudites (in the broadest sense) of Pelarda Fm. facies (Fig. 24). As for the term "rudites" we in the following will avoid this very general, somewhat diffuse and no longer often used name, and will instead speak of the more current **diamictite** (adjective: diamictic) terminology (Flint 1960 a, b) much better characterizing most volumes of the Pelarda Fm.



Fig. 24. Typical aspect of the Pelarda Fm. facies in the Salcedillo Lower S 1 part. Heterometric and polygenetic clasts in a sandy matrix.

The contact with the underlying Upper Eocene - Oligocene is concordant however erosive (Fig. 25). At a thickness of some 12 m the diamictites series exhibits various sandstone levels and lenses (Fig. 26) intercalated and a sandstone level at the top. The sequence shows a slight grading tendency with grain fining upwards, although among the individual clasts significant variations of grain sizes are observed.

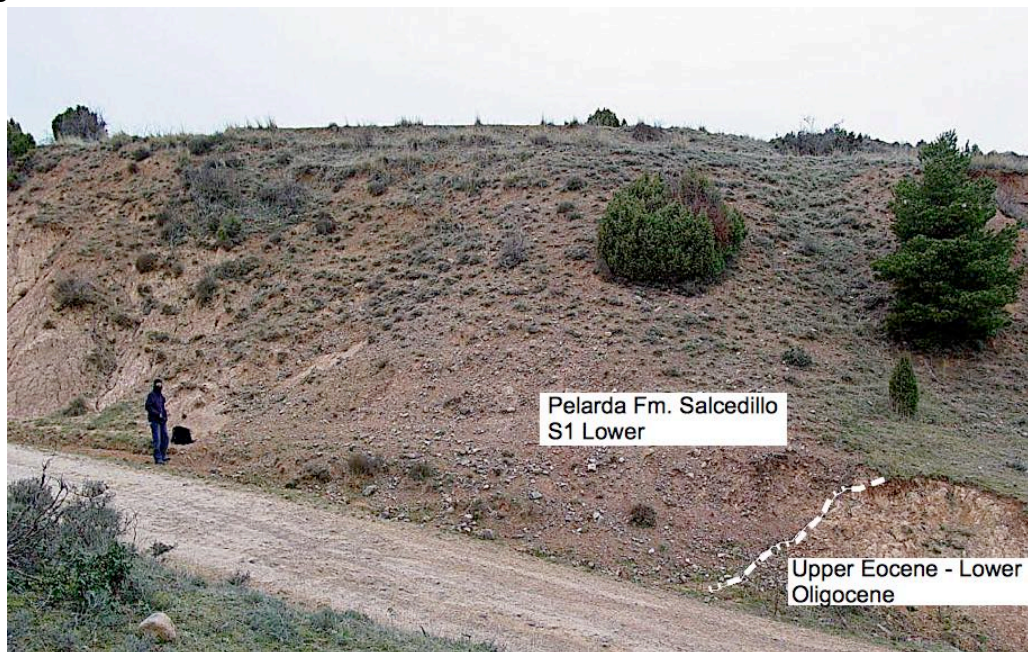


Fig. 25. Contact between the Pelarda Fm. and the Tertiary. Salcedillo S 1 Lower.



Fig. 26. Intercalated sandstone lenses within in the Salcedillo S 1 Lower diamictites.

Altogether, the diamictites are (Fig. 24)

-- polygenetic including Bámbola and Armorican quartzites, shales, schists and slates. The clast morphology varies from subangular to subrounded generally implying a low to medium sphericity.

-- heterometric with clast sizes oscillating between 1 and 35-40 cm.

-- matrix supported. Although there are scarce zones with clast-supported texture, the unit is dominated by a sandy-clayey matrix the sand having grain size between fine and coarse and compositionally being similar to the intercalated sandy levels.

Macroscopic superficial features of the clasts include subparallel open (tensile) fractures, irregular fractures with complex bifurcations (Fig. 27), and striations. Microscopically, planar features in quartz like planar deformation features, PDFs, and planar fracture, PFs, are regularly observed (Fig. 28).



Fig. 27. Quartzite clasts with open parallel (left) and irregular, bifurcating fractures.

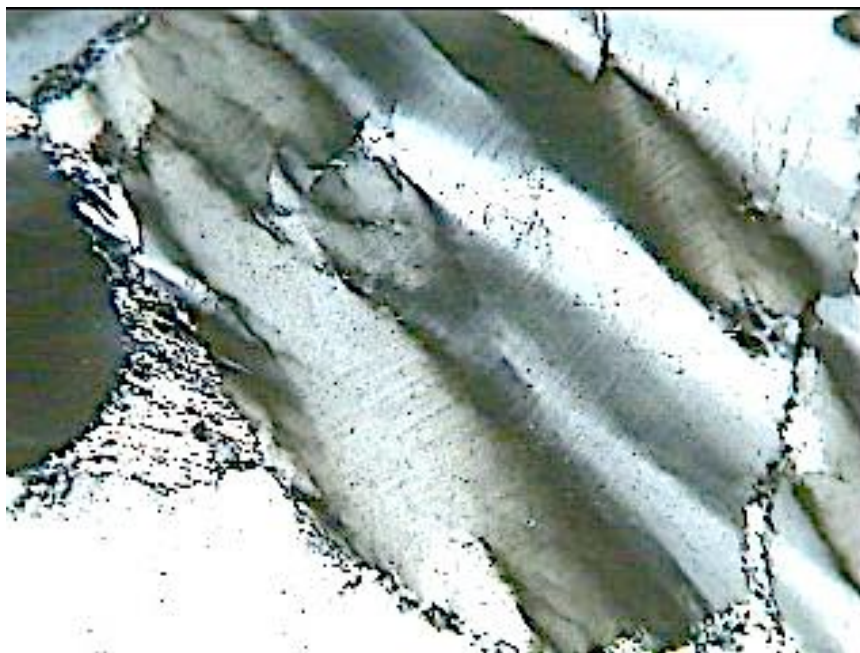


Fig. 28. Shocked quartz from the Pelarda Fm., Salcedillo S 1 Lower. Planar deformation features (PDF) and strongly kinked quartz grain with PDF.

The color of the Salcedillo S 1 unit is between reddish and yellowish-orange corresponding to the color of the underlying marly Upper Eocene-Oligocene material thus suggesting a contribution of that material to the finest fraction of the matrix of the Pelarda Fm.

In general, a certain stratification is defined by the orientation of elongated clasts (SW general dip; Fig. 29), although a chaotic layering can also be frequently observed.



Fig. 29. Elongated adjusted clasts Indicate some layering.

The sandstone levels, intercalated in the diamictic material are heterometric lithoarenites (Folk 1968) composed of quartz, schist, quartzite and slate particles with grain sizes between fine and coarse. At medium sphericity, the grain morphology varies between angular (quartz and quartzite grains) and subangular (metamorphic grains). No magnetic particles (magnet and binocular applied) were found.

The sandstone level in the top also corresponds to a heterometric and polygenetic (quartz, schist, quartzite, slate) lithoarenite (Folk 1968). Only contrasting in sphericity (medium to low) and displaying some parting lineation, the top level has the same facies as have the intercalated lithoarenites described before.

Salcedillo Intermediate S1

Between Salcedillo S1 Lower and Upper, there is a powerful silty-sandy section about 70 m thick. It is basically made up of shales with heterometric grains of quartz, quartzite (Bámbola and Armorican), and metamorphic rocks (slate and schist). The morphology of quartz grains is angular or very angular, while that of the rest is subangular. The sandy levels correspond compositionally to heterometric lithoarenites (Folk, 1968), with the same components of the larger limolites. Their morphology is similar to that of the silty-sandy levels.

Between the set of shales and sands, at the base and close to Salcedillo S 1 Inferior, a level of lenticular morphology, with a maximum thickness of 2 m and with cross bedding of low angle (Fig. 30) occurs. It contains heterometric clasts of Bámbola and Armorican quartzite and metamorphic rocks immersed in

a sandy matrix. The maximum size of the clasts does not exceed 40 cm. The contact of this level with the underlying sandstones is clearly erosive.



Fig. 30. Aspect of the middle zone. The contact with sandy sections (in white), clearly erosive, has been highlighted. The dip at this level is roughly 140/35 SE. Paleocurrents, where they have been measured, indicate a contribution from N - NE.

In addition to this diamictitic layer, there are two levels - one nearby (Fig 31) and another close to the contact with Salcedillo S 1 Upper - with a limestone appearance and slightly reddish tones (Fig. 32).



Fig. 31. The first calcareous level interspersed between the sandy materials. It has a lenticular morphology and its dip is about 140/35 SW.



Fig. 32. Detail of the "carbonate" level in Fig. 31. The yellowish zones correspond to strongly altered slate clasts.

Salcedillo Upper S1

This some 26 m thick series is made up of an alternating sequence of diamictic and sandy levels totaling nine and each grain-fining upwards. It is overlying the intermediate lithoarenite unit (Fig. 33) and covered by a few meters thick Quaternary layer (Fig. 34).



Fig. 33. The initial diamictite level of the Salcedillo S 1 Upper series is placed in erosive contact on the fine-medium grain lithoarenites of the Middle S 1 part. Note the accumulation of large clasts near the contact.



Fig. 34. The Quaternary, with horizontal or subhorizontal dip ($< 5^\circ$), lies in discordant contact with the Pelarda Fm. Its thickness never exceeds 8 m.

Each level is in general composed of a diamictic basal part (*dia*) and a sandy upper part (*ar*; see Fig. 35). In the *dia* part, also sand bodies may be intercalated.





Fig. 35. (upper and lower Figs.). Levels of sandstones (ar) and diamictites (dia) in Salcedillo S 1 Upper. In the diamictic part there is a certain tendency to a parallel arrangement to the stratification of the elongated clasts. In some points a certain incipient imbrication can be observed. cu = Quaternary.

The diamictic basal parts are

- polygenetic (Bámbola and Armorican quartzite clasts, shales, schists, Permotriassic quartzarenites (Buntsandstein Fm.) and other quartzarenites, slates). The clast morphology varies from subangular to subrounded implying a low to intermediate sphericity.
- heterometric with clast sizes between 1 and 60 cm.
- matrix supported, although there are subordinate zones exhibiting clast-supported texture. In the sandy-silty matrix the sand has grain sizes between fine and coarse and regarding composition is similar to the sandy levels.

The color tends to reddish due to quartzarenitic Buntsandstein material contributing to the deposit. In general a certain stratification is defined by the parallel disposition of the elongated clasts (Fig. 35), although there are points where it is chaotic. The general dip of the materials, where it can be measured, oscillates between about 135/40 SW and 145/30 SW. The direction of the paleocurrents indicates an origin of the N-NE.

The clasts may show rotated fractures (Fig. 36) (Ernstson & Claudin 1990), superficial striations (Fig. 37), irregular fractures with complex bifurcations (Fig. 38), and occasionally an intense polish (Fig. 39). A

measurement of the strike of the striae sets gives a preferential SW - NE direction identical to that published by Ernstson & Claudin (1990).



Fig. 36. Rotated fractures in a Bámbola quartzite.

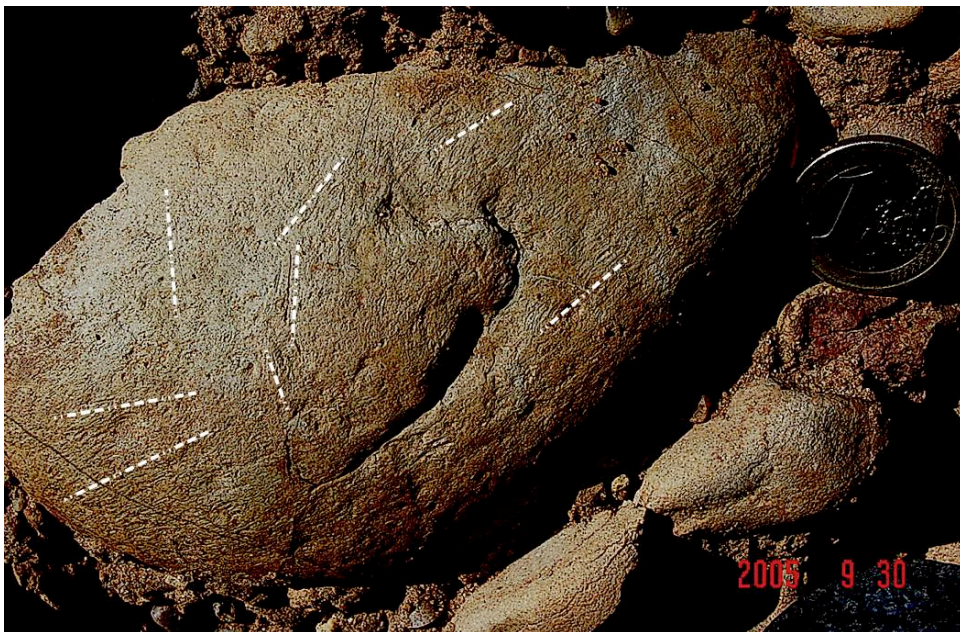


Fig. 37. A phyllite clast with multiple sets of striae.



Fig. 38 The irregular fractures and the coherence of the clast show that the rupture must have occurred in situ under high pressure, as a subsequent transport would have disassembled the sample.



Fig. 39. Bámbola quartzite clast with intense polish.

Under the microscope, thin sections of Bámbola and Armorican quartzite clasts exhibit impact metamorphic (shock) features (both PFs and PDFs).

The upper sandstone part (Fig. 35), where it has been sampled corresponds compositionally to a heterometric lithoarenite (ranging from fine to

coarse sand), with grains of quartzite, schist, phyllite, slate and quartz. Morphologically these grains range from angular (most quartz) to subangular (metamorphic rocks), presenting a low sphericity. No magnetic particles were found in any of the samples analyzed. The presence of parting lineation can be mentioned as a remarkable sedimentary structure.

A notable aspect in this section is the presence of pseudotectonic deformations, specifically tension faults that affect certain sections (sandy or diamictic parts), but without affecting all the lower or superjacent parts (Fig. 40).



Fig. 40. Pseudotectonic tension faults affect the sandy part just in front of W. Monninger, and the lower part of the next diamictic level, which however, "fossilizes" the fault by the basal clasts.

The field observations show that the mechanism is syndepositional, corresponding to a rapid sequence of erosion, sedimentation, faulting and flow within a limited unit. This type of deformation cannot be explained by "normal" geological forces, and in this particular case we refer to very similar observations in the large Rubielos de la Cérda impact basin accompanying the Azuara structure (Fig. 41) (<http://www.impact-structures.com/2011/12/cutting-into-an-impact-crater-rim-excavation-and-modification-signature-of-the-impact-cratering-process/>). Such a process (Fig. 41) is understood only by the complex movements of impact excavation, modification and location of ejecta with permanently varying strong stress and in a short period of time, probably supported by the action of shock-produced water and volatiles, which underlines the impact relationship of the Pelarda Formation. Fig. 42 shows a very simple model of this so-called *stop-and-go* deformation.

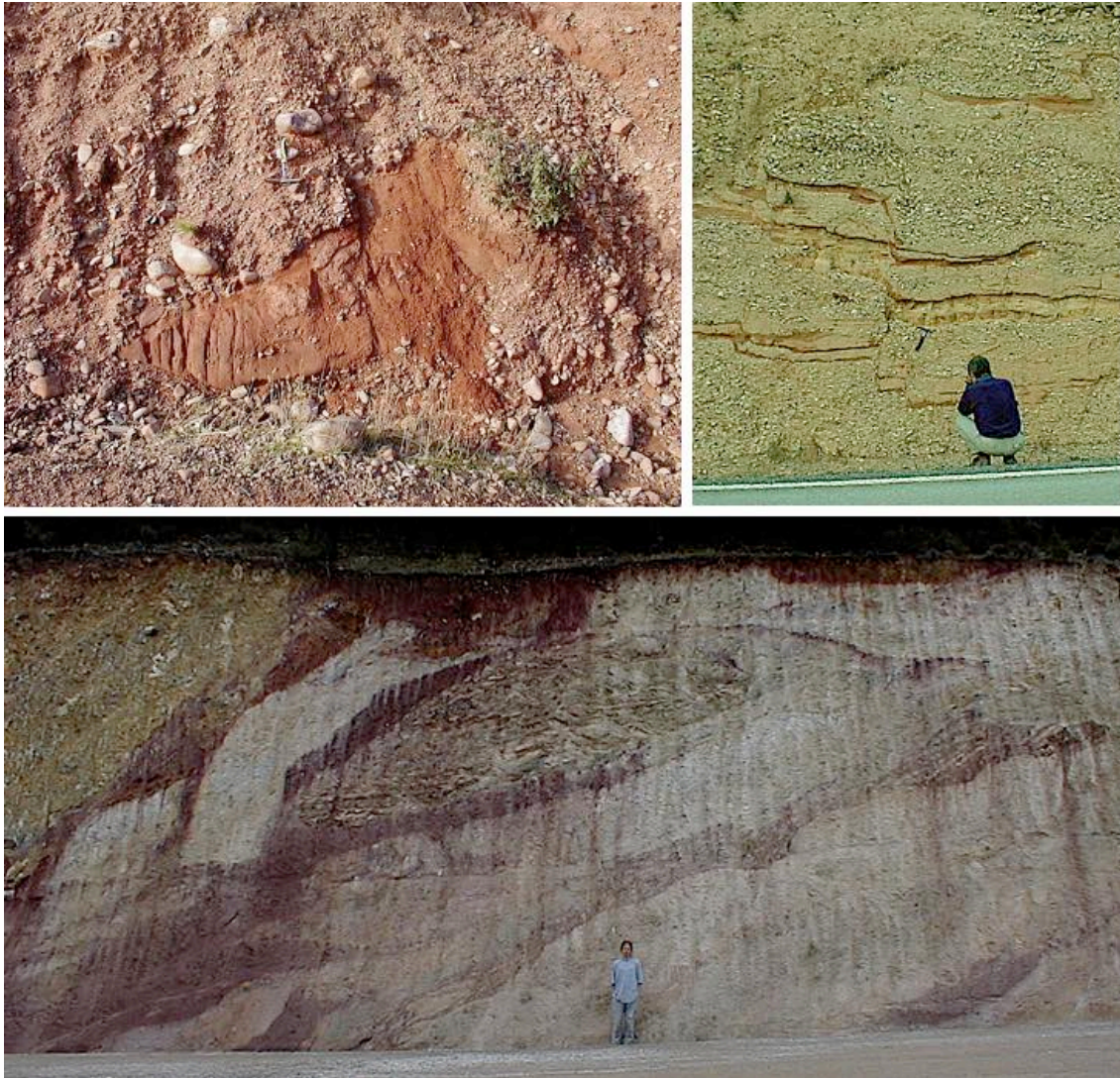


Fig. 41. *Stop-and-go* deformations in the Pelarda Fm. compared to very similar deformations in the Rubielos de la Cérída impact basin (Barrachina megabrecha, top right, and southeast rim of the basin northeast of Teruel) that emphasize this typical impact process.

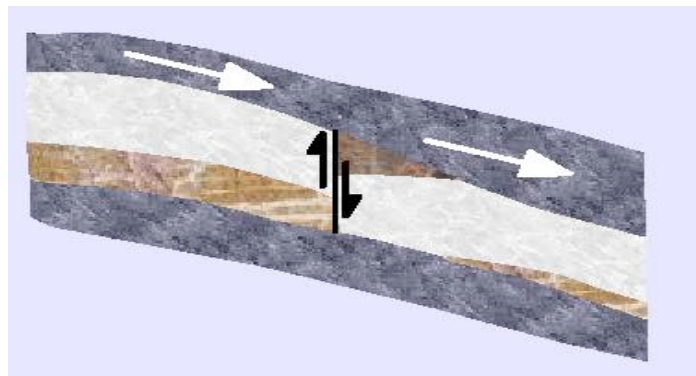


Fig. 42. Simple model for the pseudotectonic process with multiple phases typical of impact.

Salcedillo S 1, Quaternary

Wherever the Quaternary is present, it is easily identified, since its dip is practical horizontal and overlaps the aforementioned materials discordantly (Figs. 35, 35). The thickness of this cover, in the areas analysed, does not exceed 15 m in any case. Its upper part presents somewhat darker colors, due in most cases to the presence of organic matter.

4.2.2 Salcedillo S 2

Continuing along the path that goes from the village of Salcedillo to S 2 (at coordinates 30665781 E / 4533873 N (1283 m altitude), the materials that make up the upper part of the Pelarda Fm. are no longer exposed in outcrops. The study of the lithology is enabled by the farmers' ploughing of the fields (Figs. 43, 44). Evidently these materials correspond to the Pelarda Fm., since the Miocene is formed, in this zone, exclusively by breccias of Paleozoic and shale clasts (IGME, 1977; ITGE, 1989 and 1991; own field observations).



Fig. 43. Materials of the upper part of the Pelarda Formation (S 2). Buntsandstein, Bámbole quartzite, Armorican quartzite and Eocene limestones and conglomerates can be sampled in the field.



Fig. 44. Among the "waste materials", basically clasts that bother field ploughing, a clast of Eocene-Oligocene conglomerates (next to the GPS locator) as well as clasts of Bámbole quartzite, Armorican quartzite, Buntsandstein quartzite and Jurassic limestones occur.

Continuing the same path and before reaching a fork, increasing prevalence of limestone clasts changes the coloring of the fields from reddish-brown (typical of the Pelarda Fm.) to whitish-brown. After the bifurcation and according to the ITGE cartography of 1991 Miocene materials begin to appear.

4.2.3 Road from Olalla to Fonfría (S 3 and S 4 in Fig. 6 and Fig. 23)

The aspects of the S 3 and S 4 outcrops along the road between Fonfría and Olalla do not change only with altitude (see Fig. 23) but also due to its bendy course from roughly parallel to perpendicular of the strike/dip of the Pelarda Fm.

S 3 appears as a massive and diamictic aspect of the Pelarda Fm. between Fonfría, the height of Pelarda and the first 2 km of descent towards Olalla (Fig. 45).

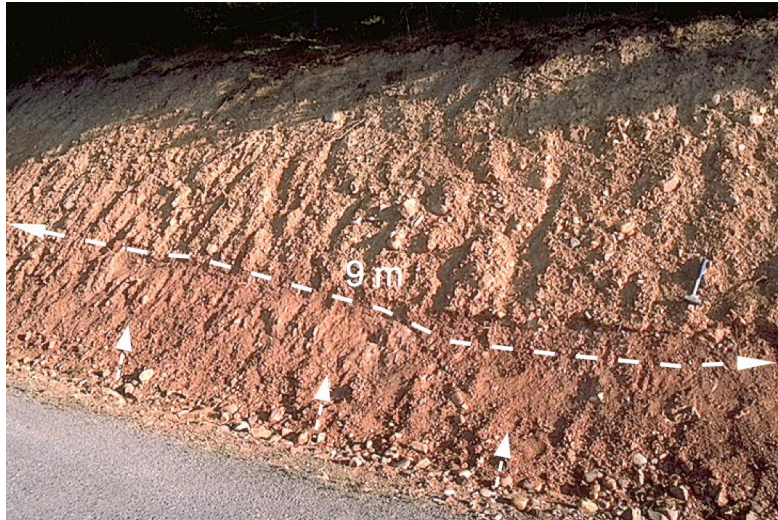


Fig. 45. Massive and diamictite-like aspect of the Pelarda Fm. along S 3. A Buntsandstein megaclast, about 9 m long, is interspersed between the materials. It should be remembered that the reddish coloration of the matrix is due to the contributions of Buntsandstein materials.

Following the road descent towards Olalla (S 4), the depositional characteristics become more similar to those observed in Salcedillo (Figs. 46, 47). Moreover advancing towards the roof of the Formation in section S 4, blocks of Bámbola quartzite bigger than 1 m (see Fig. 5, Fig. 18) with grooves and striations on its surface occur. As in Salcedillo, the clasts of the diamictic sections present rotated fractures, striae on their surface, open parallel fractures and irregular fractures with complex bifurcations. All these characteristics, already described by Ernstson & Claudin (1990), are indicative of the action of intense confining pressure at the time of deposition.

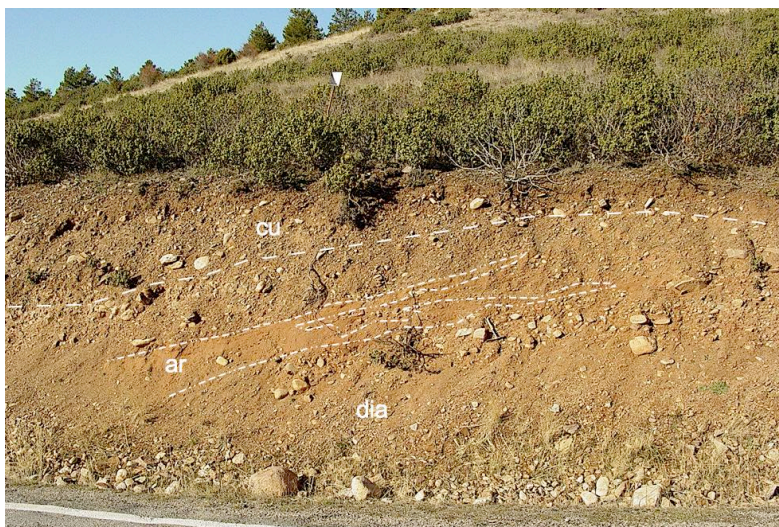


Fig. 46. Appearance of the Pelarda Fm. in the outcrops of zone 4. A sandy layer (ar) (with diamictite intercalations) is interspersed within a diamictic section (dia). The dip of the materials in this zone is 26° towards SW. qu = Quaternary.



Fig. 47. Another aspect of a diamictic part along S 4 with clasts of Armorican quartzite, metamorphic rocks and Bámbole quartzite, immersed in a sandy-loamy matrix.

A remarkable depositional situation is met in the course of S 4, in front of the Sanctuary of Pelarda, where an extended outcrop of Buntsandstein in the middle of the materials of the Pelarda Fm. was mapped by Monninger (1973) as an inverted megablock (Fig. 48, 49), indicated by inverted crossbedding.

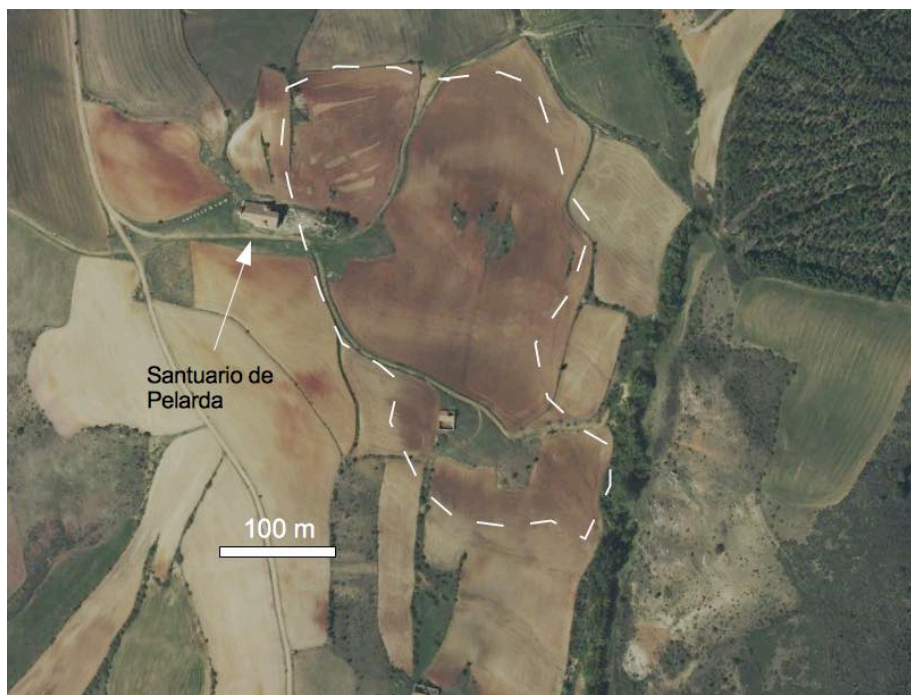


Fig. 48. The Buntsandstein block in the center of the Pelarda Formation can be recognised by its characteristic color and can therefore also be mapped in aerial photography. According to Monninger (1973) the Buntsandstein block is inverted. Aerial photography Apple Maps.



Fig. 49. Outcrop of the inverted Buntsandstein megablock that was probably transported by the Pelarda Fm. The extension of this zone is more than 300 meters (Fig. 48). Sampling in the field reveals Buntsandstein clasts with rotated fractures and impact marks (Figs. 50 and 51).



Fig. 50. Buntsandstein clast with impact collision marks (not pressure dissolution; see http://impacto.impact-structures.com/?page_id=1431) on its surface.



Fig. 51. Buntsandstein clast with rotated fractures but having remained coherent.

Altogether, moving from Fonfría to Ollala the complete sequence of the Pelarda Fm. stratigraphy can be traversed.

4.2.4 Contacts

The rim breccia

The Pelarda Formation ends up in contact with a new formation that had originally been mapped by Monninger (1973) and which he called the rim breccia (rim related to the Pelarda Formation). He divided it into a *P* rim breccia with Paleozoic components (mainly Cambrian) and an *M* rim breccia with Mesozoic components. Its distribution was mapped by Monninger (1973) as a strip extending in front of the mighty Olalla block (Claudin & Ernstson (2012) of Cambrian and Mesozoic rocks. The *P* rim breccia (Fig. 52) is formed exclusively by Paleozoic components of clayey-loamy composition with transition to quartzite sandstones and quartzite that dominate towards the road (section S 4 of our Pelarda Fm. research). The components are completely angular, a cement is missing, and the matrix contribution is very low (Fig. 53). Armorican quartzite components may have rotational fractures (Figs. 54), although no striations have been observed on their surface, possibly due to the granular surface of the quartzite. The *M* rim breccia with a similar texture was not included in our investigations, although the brecciated limestone blocks up to 1 m in size described by Monninger (1973) (Fig. 55) are also obvious. Monninger could not give a satisfactory interpretation of the origin of this breccia.

In our opinion and considering the peculiar facies and the sedimentary environment (Figs. 52-58) the rim breccia is also part of the Azuara impact ejecta.



Fig. 52. The rim breccia (Monninger 1973) located above the upper end of the Pelarda Fm., and in contact with the basal suevite breccia (Fig. 56-58).



Fig. 53 Detail of the *P* rim breccia. Photo taken at the road ahead of Olalla.



Fig. 54. Rotational fracture in a quartzite clast of the rim breccia under which the Pelarda Fm. ends. There is no fracture in the rear part.



Fig. 55. A large block of heavily brecciated limestone exposed in the transition zone from the rim breccia to the basal suevite breccia.



Fig. 56. Suevite breccia in contact with the rim breccia.



Fig. 57. Transition from the Paleozoic rim breccia to the basal suevitic breccia. Such a transition from the rim breccia deposit to the basal breccia with components originating from both the rim breccia *P* and *M* appears to be characteristic (Fig. 58).



Fig. 58. Basal suevitic breccias with dominant Mesozoic components (Keuper? on the left, Muschelkalk? on the right) exposed between the rim breccia and the Olalla block (Ernstson and Claudin 2012 URL).

General contacts (also see 3.1 Geologic setting)

Field data establish that the Pelarda Fm

- a. overlies the Paleozoic and Mesozoic materials in discordant contact (Fig. 59). This contact can be seen by following the section of the road which descends from the Pelarda top towards Olalla.



Fig. 59. The Pelarda Fm. superimposes the materials of the Paleozoic (upper right of the photograph) and those of the Mesozoic (Muschelkalk limestones intruded by the lapilli dike (see Figs. 10, 11).

b. overlies Eocene-Oligocene materials at Fonfría (Fig. 12) and by erosive contact in the zone of Salcedillo (see Fig. 25).

c. underlies Miocene and Quaternary materials in discordant contacts. The contact with the Quaternary (Figs. 34, 35, 41 and 46) is easily visible in the outcrops of Salcedillo and those located in part 4 of Fonfría-Olalla. As for the contact with the materials of the Miocene, we refer to nº 63 in ITGE (1991) and Tc33-1 A-Bb in IGME (1977) where the Pelarda Formation underlies the materials dated as "Miocene". At coordinates 30655445E / 4536964 N (next to the river towards Fonfría-Olalla, near Olalla), curiously some of these materials dated as Miocene and in discordant contact with intensively folded Palaeozoic (Fig. 60) are actually a breccia of Palaeozoic fragments (quartzites and shales), heterometric and polygenetic. In the clasts rotated fractures and deformations due to low crushing can be observed (Figs. 61).



Fig. 60. Contact (white line) between the Paleozoic and materials dated as Miocene by IGME (1977) and ITGE (1991). The red line marks the limit between an upper microbreccia a breccia below.



Fig. 61. Rotated fracture in a clast from the breccia in Fig. 67.

4.3. Granulometric and textural analyses

Studies on roundness and sphericity, according to the visual criteria of Powers (1953) and Krumbein and Sloss (1955), have been carried out on more than 150 clasts collected in the outcrops visited. In the context of this paper the results are of minor importance but may be addressed in Claudin & Ernstson 2018.

4.4 Petrographic analyses of thin sections

As mentioned in the chapter on the method used, a total of 35 thin sections of clasts of the conglomerate sections were analysed, plus 25 corresponding to the different lithoarenites of the sections carried out. The analyses covered

- the lithology and microtexture of sandstones (see 4.3),
- the presence or absence of impact (shock) metamorphism,
- the search for fossils in the fine-grained "carbonate levels".

Since the analysis (a) was already dealt with in Section 4.3 and fossils could not be clearly identified (c), the discussion is limited to (b) shock metamorphism.

Shock metamorphism (shock effects)

As for the presence of features attributable to impact metamorphism, we first refer to the analyses already carried out on samples of the formation from the outcrops between Fonfria and Olalla. The results have been published in Ernstson & Claudin (1990), Ernstson et al. (2002) and in http://estructuras-de-impacto.impact-structures.com/?page_id=123. A selection of these earlier observations is compiled in Fig. 62. This includes the comprehensive and careful analysis of the PDFs conducted in the Canadian Geological Survey by Dr. Ann Therriault (2000) (Fig. 63).

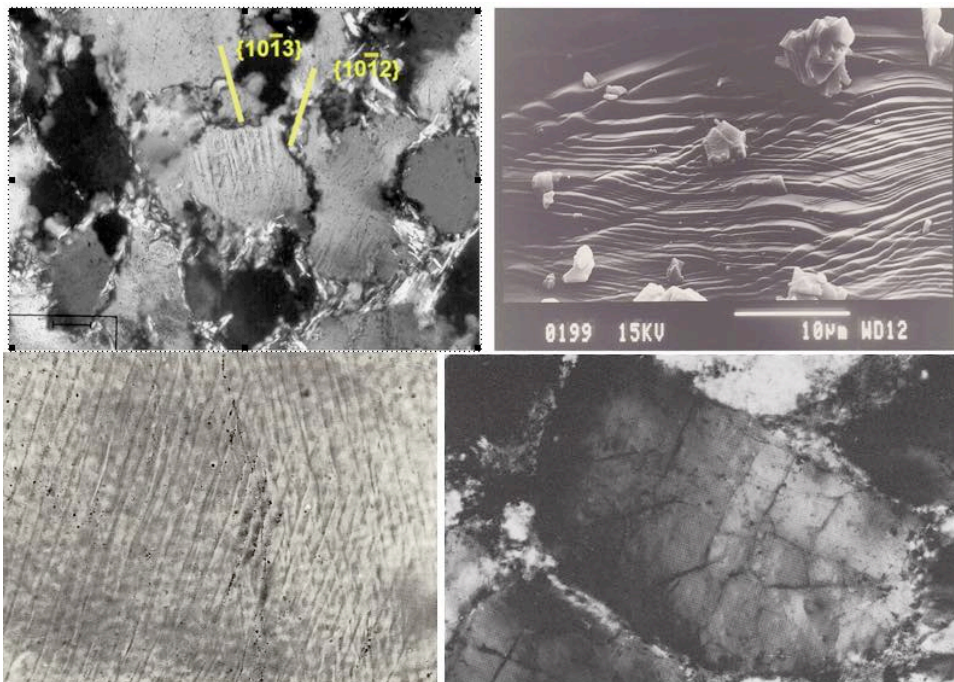


Fig. 62. Intersection of multiple sets of planar deformations (PDFs and PFs) in Pelarda Formation quartzite from previous research (Ernstson & Claudin 1990, Ernstson et al. 2002). Photo upper left: Polarization microscope, crossed polarizers (the image is 200 µm wide); right: scanning electron microscope, the PDF spacing is in part less than 1 µm. Bottom left image: two intersecting sets of PDF (image width 220 µm); bottom right image: multiple sets of planar fractures (PFs) (image width 440 µm).

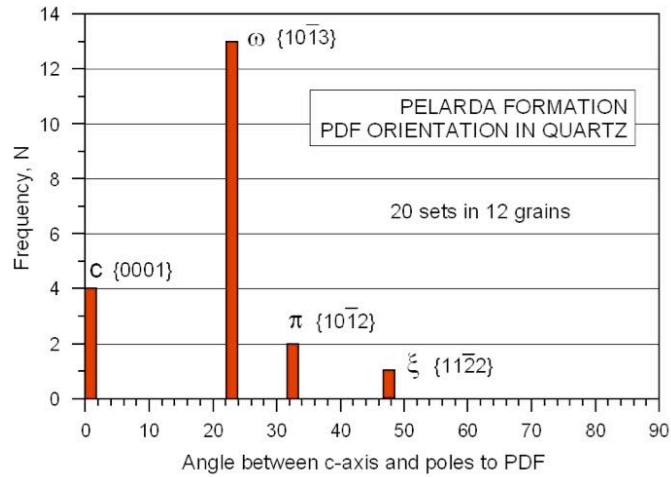


Fig. 63. Frequency diagram of the crystallographic orientation of planar deformation features (PDFs) in quartz of the Pelarda Formation. Data from Therriault (2000).

With regard to the results of the new analyses, they are in line with those previously carried out. In other words, clear shock metamorphism has been found in the case of Salcedillo (Salcedillo S 1, intermediate section, and Salcedillo S 2) clasts and in clasts from the S4 section. Planar features, both PDFs and PFs, are present in most of the quartz of the various Pelarda Fm. materials (Figs. 64, 65, 66). Identification criteria were:

- first observation under the polarizing microscope to visualize planar structures probably related to shock.
- second universal stage measurements of their orientation with respect to crystallographic planes (base c, ω , π and r).

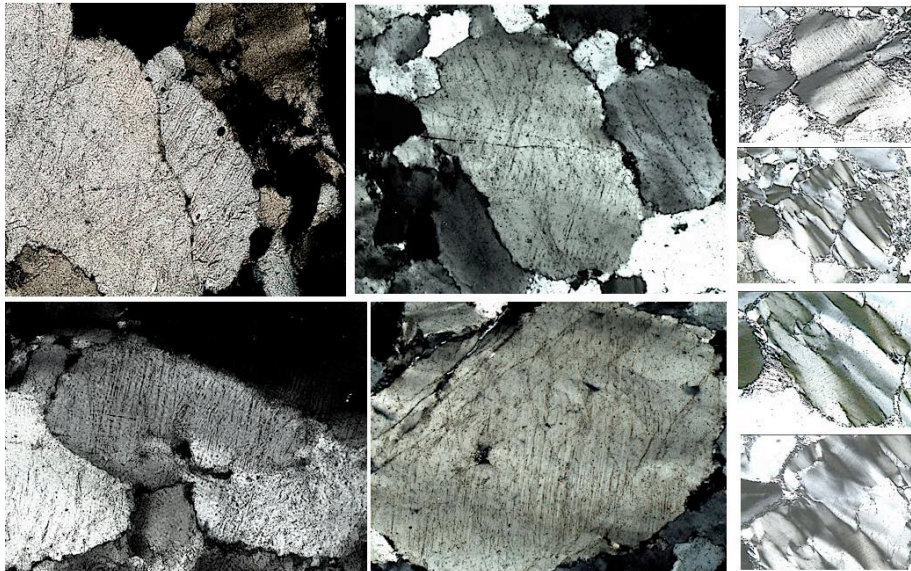


Fig. 64. Different aspects of PDFs in shocked quartz of quartzites from different locations within the Pelarda Formation. In many cases, there are several PDF systems crossing each other. Right: also considered a shock effect in quartz of the Pelarda Formation: strong kink banding with PDFs following the bands. Crossed polarizers; the images are 200 - 300 μ m wide each.

The criteria set out in French (1998) were used for previewing under a microscope. In the specific case of planar structures, among which are planar fractures (PFs) and planar deformation features (PDFs), these criteria indicate:

1. PDFs can be distinguished from cleavage and Böhm lamellae (tectonic deformation lamellae) by their width, spacing and crystallographic orientation. Cleavage consists of relatively wide ($>10\ \mu\text{m}$) and widely spaced ($\geq 20\ \mu\text{m}$) open fractures. The deformation lamellae width ranges from $10\text{-}20\ \mu\text{m}$ and they have a spacing $> 10\ \mu\text{m}$. They also show optical disorientation with respect to the grain they affect. On the contrary, PDF lamellae in quartz are highly deformed or amorphous, more or less straight (they can be curved (Trepmann & Spray, 2004, Ernstson <http://www.impact-structures.com/2011/12/are-bent-planar-deformation-features-pdfs-no-pdfs/>), which are parallel to certain crystallographic planes of the crystal they affect. Their width is small ($2\text{-}3\ \mu\text{m}$ and less) and the spacing is between $2\text{-}10\ \mu\text{m}$ or less (see Fig. 15).

2. PFs are sets of parallel fractures or cleavages with a thickness ranging from $5\text{-}10\ \mu\text{m}$ and a spacing of $15\text{-}20\ \mu\text{m}$ or more. Occasionally, planar features show typical PDF widths and are spaced between PDFs and PFs (Addison et al., 2005), the crystallographic orientation being essential for differentiation.

3. The rest of microscopic deformations produced by shock (kink bands, diaplectic glass, selective melting of minerals, ballen structures, toasted quartz), are pervasive at a centimeter scale and are developed erratically and may appear mineralogically and even grain selective.

4. While PDFs are considered indicative of impact alone, PFs are not, as they can be produced by very strong tectonic deformation. However, the development of a large number of planar fractures, widely distributed and with a small spacing, is considered as indicative of shock. In addition, multiple PF systems in a quartz grain are now considered shock and impact diagnostics (French & Koeberl 2010).

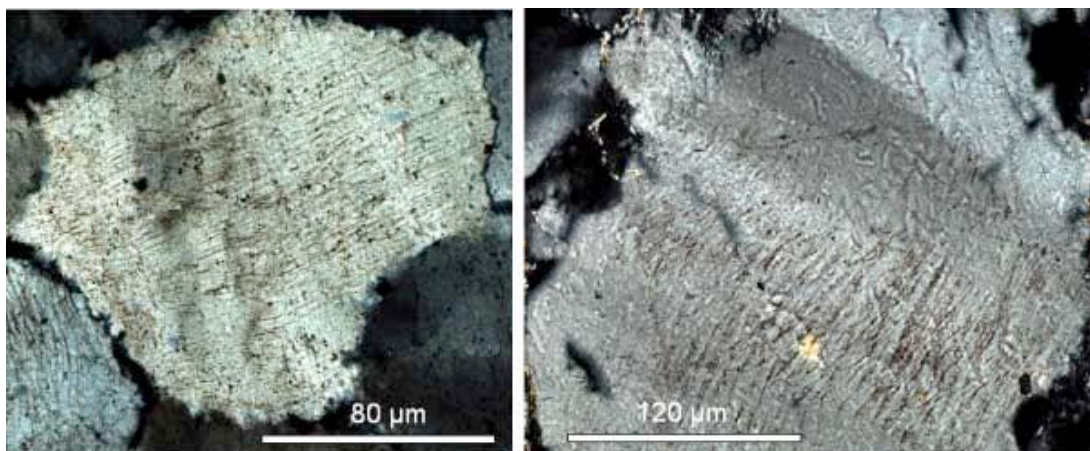


Fig. 65. Left: Curved PDFs that follow the quartz grain deformation (undulatory extinction, deformation sheets, kink bands). Right: Two PDF systems cross at a small

angle and appear to produce the image of curved PDFs. Quartz from Bámbola quartzite clasts (PDFKS2 BA-B samples).



Fig. 66. PDFs in a quartz grain from a Bámbola quartzite clast (PDFKS2 BA-B). Unlike the PDFs in Fig. 65, the PDFs appear very marked and narrow and extend along the whole grain. The difference is reasonably explained by a deformation of the quartz grains (Fig. 65) *after* the shock PDF emplacement in the contact and compression stage, when excavation and deposition of the ejected masses overprinted the quartz at high pressure.

4.5 Paleocurrent analysis

Sedimentary structures such as cross bedding, imbrication pattern of clasts, channeling and primary current lamination have been used to measure paleocurrents. The data obtained (Fig. 21) show a predominance of the NE-SW directions (mean direction N 213) defining a transport of the Pelarda Fm. deposits from NE.

4.6 Sedimentary environment

All the characteristics observed in the area of Salcedillo, as well as between the road between Fonfria and Olalla and the roads that cross the Sierra de Pelarda, establish a deposition by gravitational flows (Lowe, 1979, 1982; Colombo, 1989). The diamictic sections point to debris flows and matrix-supported clast transport *en masse* by sufficient cohesion. This transport had prevented, in most cases, clast collisions and hence preserved the abundant plastic deformations (rotated fractures, parallel fractures, fractures with complex bifurcations) and a parallel orientation of many clasts.

There are areas showing that this laminar (non-Newtonian) regime is replaced by an evolution between laminar and turbulent behavior (Enos, 1977; Nemeč and Steel, 1984; Wilson, 1980; Colombo, 1989; Colombo and Martí, 1989), mainly observed at the bases of the diamictic sections, which are clearly erosive and incorporate fragments of downwelling materials including the described megablocks along the sections S 3 and S 4. In addition, a certain tendency to internal stratification points to high-density flows with enhanced particle concentration.

The sandy sections interspersed between the diamictic sections indicate a transport in multiple stages with a sequence of "casts" (flow units) that overlapped.

An accumulation of carbonate fluids could have produced the calcareous lens-shaped intercalations in S 1 Intermediate (Fig. 31, 32) immersed within this section during transport. A karstification observed in them took place in a phase subsequent to formation. From field observations and thin-section analysis an ascription to hard-ground levels linked to lacustrine activity can be excluded. Instead we propose an origin linked with melting and decarbonization and carbonate recombination of limestone clasts in the impact event.

In the sedimentary environment of the Pelarda Fm. abundant impact indications are unmissable:

- a. macroscopic (strong plastic deformations in the clasts, shock spallation structures) and microscopic (planar structures PFs and PDFs) features.
- b. a conspicuous syndepositional failure ("*stop-and-go*")
- c. megaclasts and intercalated dislocated megablocks (up to the size of several 100 m). Here it may be added that the general trend of the Pelarda Fm. is coarsening upwards.

A summary of the observations suggests a genesis of the Pelarda Fm. deposit by successive flow units belonging to the ejecta curtain of the Azuara impact structure (Figs. A101-A108, Appendix I) and consisting of streams of semifluidized, high-density materials moving basically in a laminar flow (Schultz & Gault, 1979; Melosh, 1989; Mackaman-Lofland et al., 2014) despite some observations of turbulence.

Taking into account the lapillistone breccias, that accompany the deposit (Fig. 7), the transport agent could sometimes have been water vapour (produced in large quantities during the impact) though the general massiveness of the deposit suggests water as the predominant fluid, which was produced by the condensation of the vapour or directly excavated from the target). The vapour-liquid transitions, as well as the sudden loss of fluids within the transported mass, must have conditioned its deposition.

In this respect, the measured NE-SW striae from a frictional contact of the clasts with the matrix suggest a sudden arrest due to a loss of sustentation

in the fluid. The peculiar syndepositional faults ("*stop-and-go*") within some units can be linked to the same phenomenon.

The observed diamictite-sandstone alternation seems to reflect a tendency to pulsations within the Pelarda Fm. ejecta. Taking into account the obvious differences, they resemble those observed in volcanic pyroclastic flows and in deposits of some craters on Mars (Schultz & Gault, 1979; Melosh, 1989).

An analog line for the Pelarda Fm. would assume a flow morphology similar to a pyroclastic flow as a large drop that moves over the pre-existing surface and in which several parts can be differentiated, each of which gives rise to a characteristic deposit. As in pyroclastic flows, and depending on variations in flow velocity (sometimes influenced by topography) and on particle/fluid ratio, a whole range of transitions can be observed giving rise to different depositional facies, which in the case of massive deposits can range from debris flows to hyperconcentrated flood flows (Colombo and Martí, 1989).

4.7 Origin of the clasts

The direction and sense of the paleo-currents and the azimuth of the striae indicate an origin from N - NE. Correspondingly, the lithology of sandstone sections and the clasts of the diamictic and agrees with that of the materials (Armorican quartzite, Buntsandstein materials and others) of the S-SW part of the Azuara structure (zone of Bádenas - El Colladito - Piedrahita - Monforte de Moyuela - Rudilla - Anadón, Fig. 2), with the exception of the Bámbola quartzite clasts. Today the nearest Bámbola quartzite outcrops near Codos.

From the coexistence of rounded, subrounded, angular and subangular Paleozoic, Mesozoic and Eocen-Oligocene clasts, contributing to the Pelarda Fm., an origin can easily be settled in the Azuara impact target region where kilometer-thick molasse materials from the Pyrenees and the Iberian Chain must have been affected by the impact excavation (see Appendix I).

4.8 Age

The lower and upper limits of the Pelarda Fm., as well as the contacts allow a relative dating of the Azuara impact event and the deposition of the ejecta. Hence, the official geological maps (ITGE, 1989 and 1991; IGME, 1977), date the lower limit of the event to the Upper Eocene/Oligocene and the upper limit to the Lower Miocene. In this sense, the paleontological data published in Ernstson et al. (2002), and those of Peláez-Campomanes (1993), also confirm this age.

An absolute K-Ar dating of an impact melt rock failed because of totally unreliable ages.

4.9 More Pelarda Fm. ejecta deposits: the San Roque deposit

In recent years, with more extensive field work and mapping, we have repeatedly encountered deposits and outcrops that in many cases showed the particular characteristics of the Pelarda Fm. and in one case were so typical of the Pelarda Fm. that we add a detailed description in an Appendix II.

5. Discussion

At the beginning and referring to the investigations presented here, we unambiguously state:

The Pelarda Fm. is not a deposit of raña type, which is a glaciais of clasts with clay matrix and developed on Paleozoic soils (ITGE, 1989; ITGE, 1991; Aurell et al., 1993; Aurell, 1994; Cortés et al., 2002; Díaz-Martínez et al, 2002 a, 2002b, 2002c; Díaz-Martínez, 2005), and it is also not a fluvial deposit as originally suggested by Carls and Monninger (1974).

We discussed and justified this and summarize:

a. From the Salcedillo outcrops it is evident that the Pelarda Fm. materials are overlying Upper Eocene-Oligocene, in obviously concordant (though erosive) contact.

b. The deposition of the Pelarda Formation took place by gravity flows linked to the expansion and deposition of the Azuara impact ejecta. Fluvial sedimentation [Carls & Monninger, 1974; Adrover et al., 1982; Smit, 2000 (written communication)] is incompatible with depositional characteristics observed and described in this article. Here it is in particular worth noting that typical deformations in the diamictic levels (rotated fractures, open parallel tensile fractures and fractures with complex bifurcations) could not have survived transportation under a fluid, mostly turbulent (Newtonian) regime.

We should also address the comment of Smit (reputable sedimentologist and impact researcher, written comm. 2000) "nicely rounded pebbles which cannot originate in an ejecta deposit", which completely disregards that the roundness of many Pelarda Fm. clasts has already been brought along from the pre-impact molasse deposits in the Azuara target and that even in the excavation and ejection process and under high pressure an "impact conglomeritization" of bedded limestones (Ernstson & Claudin 2013a) could have occurred.

A basic disaccord between our observation and descriptions of the Pelarda Fm. characteristics and the depositional models of the impact opponents (alluvial fan, Miocene relations) (ITGE (1991), Cortés et al. (2002), Díaz Martínez, 2005)) is in more detail discussed in Claudin & Ernstson (2018).

Here we add the question, how to explain by fluvial processes or linked to an alluvial fan and low transport efficiency

- the presence of the Buntsandstein megablocks (Fig. 45, Fig.48),
- the Bámbola quartzite clasts bigger than meter size (Fig. 5),
- the clasts of Eocene-Oligocene materials (Fig. 43/44),
- the surface and microscopic characteristics (shock effects) of the clasts and
- the peculiar syndepositional (*stop-and-go*) faults of Fig. 40?

c. The age of the Pelarda Fm. lies between the Upper Eocene-Oligocene and the Lower Miocene. The attribution of a Quaternary age (ITGE, 1989; ITGE, 1991; Aurell et al, 1993; Aurell, 1994; Smit, 2000 (written comment), Cortés et al., 2002; Díaz-Martínez et al., 2002 a, 2002b, 2002c; Díaz-Martínez, 2005) comes into obvious, unanswerable conflict with the geologic contacts observed and described here. Also, if the Pelarda Fm. were a deposit of a Quaternary glacia, it should have developed at the feet of an abrupt relief, needing the explanation, why the Pelarda materials are exposed in top altitudes of the region. A priori, it is difficult to have a considerable uprising during the Quaternary at the same time, however making way for erosion to eliminate these reliefs. Also very strange is the assumption of tectonics so active during the Quaternary (perhaps a late "*fase Iberomanchega*" deformation) and particularly intense only in the Pelarda area.

d. Impact opponents (Cortés et al., 2002) argue that Ernstson and co-workers propose complex explanations for the predominance of Palaeozoic clasts and the practical absence of limestone in the Pelarda case, in contrast to the ejecta of the Rubielos de la Cérda impact structure in Pto. Mínguez, where carbonate rocks predominate (Ernstson et al 2002). This argument fails to recognize several factors. At the time of impact, the targets in the Azuara area and the Rubielos de la Cérda area may have been significantly different in terms of limestone and Paleozoic units. Ignored by the opponents is that in contrast to the large Pelarda Fm. distribution, the ejecta outcrops (at Puerto Mínguez) with alternating Mesozoic and Paleozoic units are relatively small, not allowing generalization. The essential factors of the impact cratering process are also overlooked, where shock propagation leads to extreme temperatures of many 1000°C following shock pressure, with the result that considerable volumes of the target evaporate and melt prior to ejection. At the relatively low temperatures at which limestones melt and/or decarbonate, this could have led to very different "destruction" or elimination of the carbonate facies in different targets. In the case of primarily different targets, the inverse stratigraphy that occurs twice could also have been an important agent: in molasse sedimentation with younger ages downwards and the following impact

excavation, in which the primary inverse layering of the molasse sediments is inverted once again ("the overturned slab" [Shoemaker]). Exactly this could be expressed in our observation that in the Salcedillo area to the top of the Pelarda F. the Jurassic and Eocene/Oligocene components visibly increase significantly.

e. In Fig. A101-A108 (Appendix I), the illustrations exemplarily show the Azuara impact cratering with the excavation, ejection and deposition of the Pelarda Fm. The sequence of images is based on publications of several computer simulations on the genesis of an impact crater. They show that the whole of the ejecta are not deposited in a single pulse, but would be the result of various thrusts of flow units.

These floods were deposited according to the ballistic erosion model of Oberbeck (1975), as streams of semifluidized and high-density materials which basically moved in a laminar flow (Schultz & Gault, 1979; Melosh, 1989). This process allowed the plastically deformed clasts (with prominent rotated fractures, parallel open tensile fractures, fractures with complex bifurcations) to survive the transport.

On occasion, the diamictic levels show erosive capacity incorporating materials from below. For comparison: Deep NASA drilling in the ejecta masses of the Ries crater ("Bunte breccia") (Hörz 1982) show that during the landing of the ejecta according to the drill core volumes up to 2/3 of the local material was scraped and incorporated by 1/3 of ejecta material. In the Pelarda case because of the dominantly water- and vapor-supported laminar, subordinately turbulent behavior, this process was less effective. The contribution of volatiles in the ejection process is suggested by the occurrence of the lapillstone breccia deposits and dikes adjacent to the Pelarda Fm. (Figs. 11) (also see Branney & Brwn (2011), Brown et al. 2010).

The vapour-liquid transitions, as well as the sudden loss of fluids in the heart of the transported mass must also have been an important agent. It was the intermittend sudden arrest of the flows, together with the intense confining pressure that produced the many striations and the in part strong polish of the clasts. The dominance of the NE-SW direction of the striations together with the measured paleocurrents is clear evidence of a relation to the Azuara impact.

A certain and not at all quantifiable erosive capacity at the base of the Pelarda Fm. as a whole is attributed to the in part strong deformations of the Eocene/Oligocene conglomerates at Fonfría, which were overrun here by the ejecta (Fig. 12, 13).

f. Due to the pre-impact topography the thickness of the Pelarda Fm. may vary from one zone to another. The maximum 200 m suggested by Carls & Monninger (1974) may according to our observations reach about twice as much (400 m). The Quaternary, where observed never exceeds 20 meters.

g. The diamictitic, disordered aspect of the Pelarda Fm. during the ascent to the height of Pelarda and the rather stratified aspect downhill relates to the curvy course of the street running parallel and perpendicular to strike/dip. The related study of the depositional character did not use the *terminology* of Miall (1978), Moncrieff (1989) or Schönian (2003) but tried to refer to their descriptions only.

h. The source area of the Pelarda Fm. materials, according to the paleocurrents and the azimuth of the striations, is located in the N-NE. The Bámbola quartzite clasts embedded in the ejecta apparently speak against this provenance (Adrover, 1982; Carls, 2005 (personal comm.)), since the Bámbola quartzite is now exposed at Codos in the NNW. As already emphasized, the composition of the ejecta material with its clasts is strongly influenced by its origin from the molasse basin targeted by the Azuara impact.

i. The distance of the Pelarda Fm. ejecta from the center of the Azuara crater, less than 2 times its radius (Cortés and Casas, 1996; Cortés et al., 2002; Díaz-Martínez et al., 2002 a and b; Díaz Martínez, 2005), is consistent with the studies that exist on proximal ejecta. According to these (French 1998), approximately half of the proximal ejecta is deposited (through various mechanisms) within 2 times the distance of the crater radius ($2R_c$) or $1R_c$ from the crater rim to form a continuous ejecta curtain that can present thicknesses from tens to hundreds of meters. Moving further away i.e. for distances $> 2 R_c$, the thickness of the ejecta is decreasing and its distribution becomes discontinuous. Practically 90% of the ejecta is deposited inside a zone defined by a circle of radius $5R_c$.

Apart from the fact that this is a very simplistic model, which depends very much on many additional factors, we mention the figures in this regard, with an Azuara structure diameter of roughly 40 km, $2R_c = 40$ km, $1R_c = 20$ km and $5R_c = 100$ km. The center of the Pelarda Fm. between Fonfría and Olalla has about 25 km distance to the center, $R_p > 1.5 * 1R_c$, in good agreement with the model data.

After this little clarification, it remains a mystery why authors Cortés and Casas, 1996; Cortés et al., 2002; Díaz-Martínez et al., 2002 a and b; Díaz-Martínez, 2005 present a scheme of the Azuara structure with two circles and radii of $1R_c$ and $2R_c$ respectively, claiming and insisting that the location of the Pelarda Fm. excludes an origin as ejecta. We assume that they have never read the corresponding literature on proximal ejecta.

6 Conclusions

After more than 20 years of discussion about the Pelarda Fm., after the early works of Monninger (1973) and Carls & Monninger (1974), with numerous publications of the impact proponents and impact opponents, as well as detailed contributions of the three current authors on the Internet pages www.impact-

structures.com, here for the first time an extensive article in English language including our recent investigations is presented, after an extended version already appeared in Spanish language (Claudin & Ernstson (2018). To this must be added the activities of some leading impact researchers of the so-called "impact community", who still ignore the Azuara impact event, which, apart from the strict rejection by Spanish regional geologists, has also contributed to the fact that even in the most recent literature on Spanish geology this striking geological event still does not take place.

In addition we conclude that with the observations, measurements, analyses and descriptions presented here in detail, all claims of the impact opponents can be refuted easily. We attribute the attitude of the opponents to a lack of field work, the reliance on outdated literature, a lack of knowledge of elementary and generally accepted impact criteria and, above all, to a general rejection of a major impact event in a region, in which generations of geologists have produced many thick theses, doctoral theses and extensive publications regarding conventional regional textbook geology only. Such a constellation has existed in principle for decades and still exists today all over the world, when regional geologists are suddenly confronted with the completely new situation of a postulated impact structure. In this Azuara case we wonder however that after 20 years of scientific evidence of impact, there is still a lack of scientific insight.

Whether this article will change the opinion of the persons addressed remains questionable, but it should familiarize the more open-minded international impact research community with one of the greatest terrestrial impact ejecta occurrences and, if necessary, initiate a discussion.

Acknowledgements. We thank P. Carls, who has worked for decades since the sixtieth in the region of the Paleozoic of the Eastern Iberian Chain, for many discussions about the Azuara impact and the Pelarda Fm., although we were unable until today to convince him of the reality of the big impact. We thank Pepe for years and years of really great hospitality as principal of the among geologists famous "Legido" hotel, bar and restaurant in Daroca.

References

- Addison, W. , Brumpton, G.R., Vallini, D.A., McNaughton, N.J., Davis, D.W., Kissin, S.A., Fralick, P.W., Hammond, A.L. (2005): Discovery of distal ejecta from the 1850 Ma Sudbury impact event. *Geology*, March 2005; v. 33, nº 3 : 193-196.
- Adrover, R., Freist, M., Hugueney, M., Mein, P. & Moissenet, E. (1982): L'âge et la mise en relief de la formation detritique culminante de la Sierra Pelarda (Prov. Teruel, Espagne). *C.R. Acad. Sc. Paris*, 295: 231-236.

- Artemieva, N.A., Wünnemann, K., Krien, F., Reimold, W.U., and Stöffler, D., 2013, Ries crater and suevite revisited—Observations and modeling: Part II: Modeling: *Meteoritics & Planetary Science*, v. 48, p. 590–627,.
- Aurell, M., González, A., Pérez, A., Guimerà, J., Casas, A. & Salas, R. (1993). Discusión of “The Azuara impact structure (Spain): New insights from geophysical and geological investigations” by K. Ernstson & J. Fiebag. *Geologische Rundschau*. 82: 750-755.
- Aurell, M. (1994). Discusión sobre algunas de las evidencias presentadas a favor del impacto meteorítico de Azuara. In: *Extinción y registro fósil* (E. Molina, ed.). Cuadernos interdisciplinarios. 5: 59-74. Seminario Interdisciplinar de la Universidad de Zaragoza. Zaragoza.
- Branney, M.J., and Brown, R.J., 2011, Impactoclastic density current emplacement of terrestrial meteorite-impact ejecta and the formation of dust pellets and accretionary lapilli: Evidence from Stac Fada, Scotland: *Journal of Geology*, v. 119, p. 275–292.
- Brown, R.J., Branney, M.J., Maher, C., and DávilaHarris, P. (2010) Origin of accretionary lapilli within ground-hugging density currents: Evidence from pyroclastic couplets on Tenerife: *Geological Society of America Bulletin*, v. 122, p. 305–320.
- Carls, P. & Monninger, W. (1974): Ein Block-Konglomerat im Tertiär der östlichen Iberischen Ketten (Spanien). *Neues Jahrbuch für Geologie und Paläontologie, Abhandlungen*, 145: 1-16.
- Carrasco-Velázquez, B. , Morales-Puentes, P., Cienfuegos, E. y Lozano-Santacruz, R (2004): Geoquímica de las rocas asociadas al paleokarst cretácico en la plataforma de Actopan: evolución paleohidrológica. *Revista Mexicana de Ciencias Geológicas*, v. 21, nº 3: 382-396.
- Chao, E. Ch. (1977): The Ries crater of southern Germany, a model for large basins on planetary surfaces, *Geologisches Jahrbuch*, A43: 3-81.
- Claudin, K., Ernstson, K., Rampino, M.R., and Anguita, F. (2001). Striae, polish, imprints, rotated fractures, and related features in the Puerto Mínguez impact ejecta (NE Spain). Abstracts, 6th ESF IMPACT workshop, Impact Markers in the Stratigraphic record, pp 15-16.
- Claudin, F. & Ernstson, K. (2003): *Geología Planetaria y Geología Regional: El debate sobre un impacto múltiple en Aragón*. *Enseñanza de las Ciencias de la Tierra*, 2003 (11.3): 202-212.
- Claudin, F. & Ernstson, K. (2012): Azuara impact structure: The Daroca thrust geologic enigma – solved? A Ries impact structure analog. URL <http://www.impact-structures.com/2012/09/azuara-impact-structure-the-daroca-thrust-geologic-enigma-solved/>
- Claudin, F. & Ernstson, K. (2018): La formación Pelarda: eyecta de la estructura de impacto de Azuara (España): características deposicionales, edad y génesis. URL <http://estructuras-de-impacto.impact-structures.com/wp-content/uploads/2018/09/Pelarda-final-rudita-corrected-Komprimiert.pdf>.

- Cohen, A.S. (1982): Paleoenvironments of root casts from the Fora Formation, Kenia. *Jour. Sed. Petrology*, 52 (3): 401-414.
- Colombo, F. (1989): Abanicos aluviales. In: A. Arche (coord): *Sedimentología*, CSIC, vol. I: 143-218.
- Colombo, F y Martí, J. (1989): Depositos volcano-sedimentarios. In: A. Arche (coord): *Sedimentología*, CSIC, vol. I: 271-345.
- Cortés, A.L. & Casas,-Sainz, A.M. (1996): Deformación Alpina de zócalo y cobertera en el borde norte de la Cordillera Ibérica (Cubeta de Azuara-Sierra de Herrera). *Revista de la Sociedad Geológica de España*, 9: 51-66.
- Cortés, A.L., Díaz-Martínez, E., Sanz-Rubio, E., Martínez-Frías, J. & Fernández, C (2002). Cosmic impact versus terrestrial origin of the Azuara structure (Spain): A review. *Meteoritics Planet. Sci.* 37: 875-894.
- Diaz Martínez, E., Cortés, A.L., Martínez Frías, J. (2002 a): Tectonic and sedimentary evidence refutes an impact hypothesis for the Azuara structure, Spain, Program, Abstracts and fieldtrip Book of the 8th Workshop of ESF IMPACT Programme, Mora: p. 17.
- Diaz Martínez, E., Martínez Frías, J., Sanz Rubio, E. (2002b): Impact cratering record in Spain: a review of recent results. *Resúmenes Primer Congreso Ibérico sobre Meteoritos y Geología Planetaria*, Cuenca: p. 34-35.
- Diaz Martínez, E., Sanz Rubio, E. & Martínez Frías, J. (2002c): Sedimentary record of impact events in Spain. In: C. Koeberl & K.G. MacLeod (eds.): *Catastrophic Events and Mass Extinctions: Impacts and Beyond*. Geological Society of America Special Paper, 356: 551-562.
- Diaz Martínez, E. (2005): Registro geológico de eventos de impacto meteorítico en España: revisión del conocimiento actual y perspectivas de futuro. *Journal of Iberian Geology* 31 (1): 65-84.
- Enos, P (1977): Flow regimes in Debris-flow. *Sedimentology*, 24: 133-142.
- Ernstson, K. & Claudin, F. (1990). Pelarda Formation (Eastern Iberian Chains, NE Spain): Ejecta of the Azuara impact structure. *N. Jb. Geol. Paläont. Mh.* 1990: 581-599.
- Ernstson, K. & Fiebag, J. (1992). The Azuara impact structure: New insights from geophysical and geological investigations. *Geol. Rundschau.* 81: 403-427.
- Ernstson, K., Claudin, F., Schüssler, U., Anguita, F, and Ernstson, T. (2001): Impact melt rocks, shock metamorphism, and structural features in the Rubielos de la Cérda structure, Spain: evidence of a companion to the Azuara impact structure. Abstracts, 6th ESF IMPACT workshop, Impact Markers in the Stratigraphic record, pp. 23-24, 2001.
- Ernstson, K., Claudin, F., Schüssler, U. & Hradil, K. (2002). The mid-Tertiary Azuara and Rubielos de la Cérda paired impact structures (Spain). *Treballs del Museu de Geologia de Barcelona.* 11: 5-65.
<https://www.raco.cat/index.php/TreballsMGB/article/viewFile/72446/254637>

- Ernstson, K., Schüssler, U., Claudin, F. & Ernstson, T. (2003). An impact crater chain in northern Spain. *Meteorite*, 9, no 3, 35-39.
- Ernstson, K. (2004). Regmaglypts on clasts from impact ejecta. *Meteorite*, 10, no 1, 41-42.
- Ernstson & Claudin (2013a): The Weaubleau impact structure “round rocks” (“Missouri rock balls”, “Weaubleau eggs”): possible analogues in the Spanish Azuara/Rubielos de la Cérída impact structures. <http://www.impact-structures.com/2013/07/the-weaubleau-impact-structure-round-rocks-missouri-rock-balls-weaubleau-eggs-possible-analogues-in-the-spanish-azuara-rubielos-de-la-cerida-impact-structures/>
- Ernstson & Claudin (2013b): Reminder: Manipulation in science - “The convincing identification of terrestrial meteorite impact structures: What works, what doesn't, and why”. <http://www.impact-structures.com/2017/11/the-convincing-identification-of-terrestrial-meteorite-impact-structures-what-works-what-doesnt-and-why/>
- Ernstson, K. (2014): Meteorite impact spallation: from mega- to micro-scale. <http://www.impact-structures.com/impact-educational/meteorite-impact-spallation-from-mega-to-micro-scale/>
- Folk, R (1968): *Petrology of Sedimentary rocks*. Ed. Hemphill's: Austin. 170pp.
- French B. M. (1998) *Traces of Catastrophe: A Handbook of Shock-Metamorphic Effects in Terrestrial Meteorite Impact Structures*. LPI Contribution No. 954, Lunar and Planetary Institute, Houston. 120 pp.
- French, B.M. & Koeberl, C (2010): The convincing identification of terrestrial meteorite impact structures: What works, what doesn't, and why. *Earth Science Reviews*, Volume 98, Issue 1, p. 123-170.
- García-Ramos, J.C., Valenzuela, M. & Suárez de Centi, C. (1989): *Sedimentología de las huellas de actividad orgánica*. In: A. Arche (coord): *Sedimentología*, CSIC, vol. II: 261-342.
- Glikson, A.Y. (2005): Geochemical and isotopic signatures of Archaean to Palaeoproterozoic extraterrestrial impact ejecta/fallout units. *Australian Journal of Earth Sciences* 52(4):785-798.
- Glikson, A., Hickman, H., Evans, N.J., Kirkland, C.L., Park, J-W., Rapp, R., & Romano, S. (2016): A new 3.46 Ga asteroid impact ejecta unit at Marble Bar, Pilbara Craton, Western Australia: A petrological, microprobe and laser ablation ICPMS study.
- Glikson, A. Y., & Pirajno, F. (2018). Australian Asteroid Ejecta/Fallout Units. In Y. Dilek, F. Pirajno, & B. Windley (Eds.), *Asteroids impacts, crustal evolution and related mineral systems with special reference to Australia* (Vol. 14, pp. 31-59). (Modern Approaches in Solid Earth Sciences; Vol. 14). Springer. https://doi.org/10.1007/978-3-319-74545-9_2
- Grieve, R. A. F. & Shoemaker, E. M. (1994): The record of past impacts on Earth. In: T. Gehrels, *Hazards Due to Comets and Asteroids* (eds.): *Space Science Series*. Univ. Arizona Press, Tucson, Arizona, USA 1994, p. 417–462.

- Haines, P.W., 2005. Impact cratering and distal ejecta: the Australian record. *Aust. J. Earth Sci.* 52, 481–507.
- Hassler, S.W., Bruce M. Simonson, B.M., Dawn Y. Sumner, D.Y. & Bodin, L. (2011) Paraburdoo spherule layer (Hamersley Basin, Western Australia): Distal ejecta from a fourth large impact near the Archean-Proterozoic boundary
- Heward, A.P. (1978): Alluvial fan sequence and megasequence models: with examples from Westphalian D Stephanian B coalfields, northern Spain. In: Miall, A.D. ed., *Fluvial Sedimentology*. Canadian Society of Petroleum Geologists, Memoir 5: 669-702.
- Hodge, P. (2010): *Meteorite Craters and Impact Structures of the Earth*. Cambridge University Press, 136 p.
- Horton, J.W., Aleinikoff, J.N., Kunk, M.J., Gohn, G.S., Edwards, L.E., Self-Trail, J.M., Powars, D.S., Izett, G.A. (2005) Recent research on the Chesapeake Bay impact structure, Impact debris and reworked ejecta. *Geological Society of America Special Paper*, 384, 147-170.
- Horton, J.W. & Izett, G.A. (2006) Crystalline-rock ejecta and shocked minerals of the Chesapeake Bay impact structure, USGS-NASA Langley core, Hampton, Virginia, with supplemental constraints on the age of impact. *USGS professional paper* 1688, E1-E30.
- Hörz, F. (1982). Ejecta of the Ries Crater, Germany. In: *Geological Implications of Impacts of Large Asteroids and Comets on the Earth* (L.T. Silver and P.H. Schultz, eds.), *Geol. Soc. Amer., Spec. Pap.*, 190: 39-55.
- Housen, K.R. & Holsapple, K.A. (2011) Ejecta from impact craters. *Icarus*, 211, 856-875.
- Hradil, K., Schüssler, U., and Ernstson, K. (2001): Silicate, phosphate and carbonate melts as indicators for an impact-related high-temperature influence on sedimentary rocks of the Rubielos de la Cérida structure, Spain. *Abstracts, 6th ESF IMPACT workshop, Impact Markers in the Stratigraphic record*, pp. 49-50, 2001.
- Hüttner, R. (1969): *Bunter Trümmernmassen und Suevit*. *Geologica Bavarica*, 61, 142-200.
- IGME (1977): Memoria hoja nº 492 (Segura de los Baños) del Mapa Geológico de España. 1:50000.
- ITGE (1989): Memoria hoja nº 466 (Moyuela) del Mapa Geológico de España. 1:50000.
- ITGE (1991). Memoria hoja nº 40 (Daroca) del Mapa Geológico de España. 1:200000
- Krumbein, W.C. & Sloss, L.L. (1955): *Stratigraphy and Sedimentation*. Ed. Freeman & Co. : San Francisco. 497 pp.
- Lendínez, A., Ruiz, V. & Carls, P. (1989): Mapa y memoria explicativa de la hoja 439 (Azuará) del Mapa Geológico de España a escala 1:50000. ITGE. Madrid. 42 pp.
- Lowe, D.R. (1979): Sediment gravity flows: Their classification and some problems of application to natural flows and

- deposits. In: L.J. oyle & D.H. Pilkey (eds.): Soc. Econ. Paleont. Miner. Special Public., 27: 75- 82.
- Lowe, D.R. (1982): Sediment gravity flows II. Depositional models with special reference to the deposits of high-density turbidity currents. *Jour. of Sedimentary Petrology*, 52 (1): 279-297.
 - Mackaman-Lofland, Ch., Brand, B., Taddeucci, J. & Wohletz, K (2014): Sequential Fragmentation / Transport Theory, Pyroclast Size-Density Relationships, and the Emplacement Dynamics of Pyroclastic Density Currents – A Case Study on the Mt. St. Helens (USA) 1980 Eruption. *Journal of Volcanology and Geothermal Research* (2014), doi: 10.1016/j.jvolgeores.2014.01.016
 - McGowen, J.H. & Groat, C.G. (1971): Van Horn Sandstone, West Texas, an alluvial fan model for mineral exploration. *Texas Bureau of Economic ecology Report of Investigations*, 72: 57 pp.
 - Melosh, H.J. (1989): *Impact cratering: A geologic process*. New York: Oxford University. 245 pp.
 - Meyer, C., Artemieva, N., Stöffler, D., Reimold, W.U., and Wünnemann, K., (2008): Possible mechanisms of suevite deposition in the Ries Crater, Germany: Analysis of Otting drill core, in *Proceedings of the Large Meteorite Impacts and Planetary Evolution Conference IV: Houston, Texas, Lunar and Planetary Institute Contribution 1423*, paper 3066, 2 p.
 - Meyer, C., Jébrak, M., Stöffler, D., and Riller, U. (2011) Lateral transport of suevite inferred from 3D shape-fabric analysis: Evidence from the Ries impact crater, Germany: *Geological Society of America Bulletin*, v. 123, p. 2312–2319.
 - Miall, A.D. (1978): Lithofacies types and vertical profiles models in braided river deposits: a summary. In: Miall, A.D. ed., *Fluvial Sedimentology*. Canadian Society of Petroleum Geologists, Memoir 5, p. 567-604.
 - Moncrieff, A.C.M. (1989): Classification of poorly sorted sedimentary rocks. *Sedimentary Geology*, 65: 191-194.
 - Monninger, W. (1973): *Erläuterungen zur geologischen Kartierung im Gebiet um Olalla (Prov. Teruel) (NE-Spanien)*, Diploma Thesis, Univ. Würzburg, 140 pp.
 - Nemeč, W. & Steel, R.J. (1984): Alluvial and coastal conglomerates: Their significant features and some comments on gravely mass flow deposits. In: E.H. Koster & R. Steel (eds.): *Sedimentology of Gravels and Conglomerates*. Can. Soc. Petr. Geol., Mem. 10: 1-31.
 - Newsom HE, Graup G, Sowards T, Keil K (1986): Fluidization and hydrothermal alteration of the suevite deposit at the Ries Crater, West Germany, and implications for Mars. *J Geophys Res* 91: E239–E251.
 - Norton, O.R. (2002): *The Cambridge Encyclopedia of Meteorites*. Cambridge University Press, 354 p.
 - Oberbeck, V.R. (1975) The role of ballistic erosion and sedimentation in lunar stratigraphy. *Geophys. and Space Phys.*, 13: 337-362.

- Oberbeck, V.R., Marshall, J.R. & Aggarwal, H. (1993): Impacts, Tillites, and the Breakup of Gondwanaland. NASA Publications. 74. <http://digitalcommons.unl.edu/nasapub/74>.
- Osinski G. R., Grieve R. A. F., and Spray J. G. (2004). The nature of the groundmass of surficial suevites from the Ries impact structure, Germany, and constraints on its origin. *Meteoritics and Planetary Science* 39:10:1655–1684.
- Osinski G. R., Spray J. G., and Lee P. (2005): Impactites of the Houghton impact structure, Devon Island, Canadian High Arctic. *Meteoritics & Planetary Science* 40:12:1789–1812.
- Osinski, G.R., Tornabene, L.L. & Grieve, R.A.F. (2011) Impact ejecta emplacement on terrestrial planets. *Earth Planet. Sci. Let.*, 310, 167-181.
- Osinski, G.R., Grieve, R.A.F. & Tornabene, L.L. (2013) Excavation and impact ejecta emplacement. In: *Impact Cratering: Processes and Products*, G. R. Osinski and E. Pierazzo (ed.). Blackwell Publishing Ltd.
- Peláez-Campomanes, P. (1983): Micromamíferos del Paleógeno continental español: Sistemática, Biocronología y Paleoecología. Tesis doctoral, Universidad Complutense de Madrid, 385 pp.
- Pérez, A., Muñoz, A., González, A., Pardo, G. & Villena, J. (1989): Interpretación tectonosedimentaria de la Depresión Terciaria de Azuara. Margen Ibérico de la cuenca del Ebro. Provincia de Zaragoza. *Actas I Cong. Grupo Esp. Terc.*, 229-232.
- Pope, K.O., Ocampo, A.C., Fischer, A.G., Alvarez, W., Fouke, B.W., Webster, C.L., Vega, F.J., Smit, J., Fritsche, A.E., Claeys, P. (1999) Chicxulub impact ejecta from Albion Island, Belize. *Earth Planet Sci. Let.*, 170, 351-364.
- Pope, K.O., Ocampo, A.C., Fischer, A.G., Vega, F.J., Ames, D.E., King, D.T., Jr., Fouke, B.W., Wachtman, R.J., and Kletetschka, G., 2005, Chicxulub impact ejecta deposits in southern Quintana Roo, México, and central Belize, in Kenkmann, T., Hörz, F., and Deutsch, A., eds., *Large meteorite impacts III: Geological Society of America Special Paper 384*, p. 171–190.
- Powers, M.C. (1953): A new roundness scale for sedimentary particles. *Journal of Sedimentary Petrology*, vol 23: 117-119.
- Rampino, M.R. (2017): Are Some Tillites Impact-Related Debris-Flow Deposits? *The Journal of Geology*, 125, 105-164.
- Rampino, M. R., Ernstson, K., Anguita, F., & Claudin, F. (1997a). Striations, polish, and related features of clasts from impact-ejecta deposits and the "tillite problem". Abstracts, Conference on Large Meteorite Impacts and Planetary Evolution, Sudbury, Ontario, Canada p. 47.
- Rampino, M. R., Ernstson, K., Anguita, F., Claudin, F., Pope, K.O., Ocampo, A., & Fischer A. G. (1997b). Surface features of clasts from impact-ejecta deposits and the "tillite problem". Abstracts with Prog. Geological Society of America. 29.
- Reiff, W. (1978) Monomict movement breccias; an indicator of meteorite impact. *Meteoritics*, 13: 605-609.

- Reimold, W.U., Von Brunn, V. & Koeberl, C. (1997): Are Diamictites Impact Ejecta?—No Supporting Evidence From South African Dwyka Group Diamictite. *The Journal of Geology*, 105, 517-530.
- Schönian, F. (2003): Ambiente sedimentario de las diamictitas de la Formación Cancañiri en el área de Sella, sur de Bolivia. *Revista Técnica de YPF*, 21: 131-146.
- Schüssler, U., Hradil, K., Ernstson, K. (2002): Impact-related melting of sedimentary target rocks of the Rubielos de la Cérida structure in Spain. *Berichte der Deutschen Mineralogischen Gesellschaft, Beiheft 1 zum European Journal of Mineralogy*, Vol. 14, S. 149.
- Schulte, P. & Kontny, A. (2005) Chicxulub ejecta at the Cretaceous-Paleogene (KP) boundary in Northeastern Mexico. In Kenkmann, T., Hörz, F., and Deutsch, A., eds., *Large meteorite impacts III: Geological Society of America Special Paper 384*, p. 191–221.
- Schultz, P.H. & Gault, D.E. (1979): Atmospheric effects on Martian ejecta emplacement. *J. Geophys. Res.*, 84: 7669-7687.
- Siegert, S., Branney, M.J. & Hecht, L. (2017): Density current origin of a melt-bearing impact ejecta blanket (Ries suevite, Germany). *Geology*, 45(9): 855-858.
- Stöffler, D., Artemieva, N.A., Wünnemann, K., Reimold, W.U., Jacob, J., Hansen, B.K., and Summerson, I.A.T., 2013, Ries crater and suevite revisited—Observations and modeling part I: Observations: *Meteoritics & Planetary Science*, v. 48, p. 515–589.
- Strycker, P.D., Chanover, N., Miller, Ch., Hermalyn, B., Suggs, R.M & Suusman, M. (2013): Characterization of the LCROSS impact plume from a ground-based imaging detection. *Nature Communications* 4, Article number: 2620 (2013). Doi:10.1038/ncomms3620.
- Therriault, A. (2000): Report on Azuara, Spain, PDFs, 31 p.
- Trepmann, C.A. & Spray, J.G. (2004): Post-shock crystal-plastic processes in quartz from crystalline target rocks of the Charlevoix impact structure. *Abstracts Lunar and Planetary Science XXXV*, #1730.pdf.
- Wilson, L. (1980): Relationships between pressure, volatile content and ejecta velocity in three types of volcanic explosin. *J. Volc. Geot. Res.*, 8:297-313.

Appendix I: The Azuara impact cratering process and ejecta formation in eight images - schematic

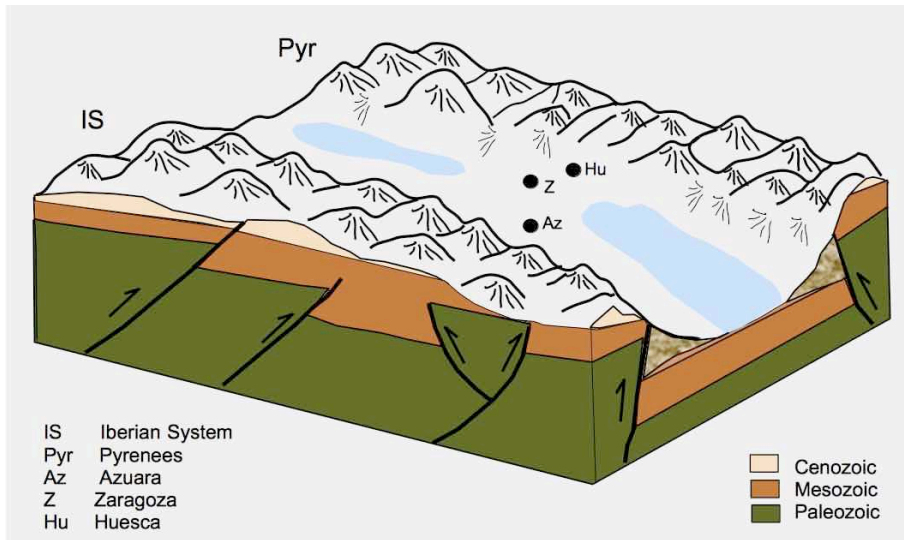


Fig. A101. Block diagram of the Azuara zone corresponding to the Upper Eocene-Oligocene period based on data from different sources. The Azuara zone would be located within an endorheic basin where materials from the erosion of the Iberian mountain range and the Pyrenees were deposited. This deposition was linked to sets of alluvial fans. The blue colour corresponds to areas of lagoons and lakes formed by the accumulation of water from these two large mountain masses.

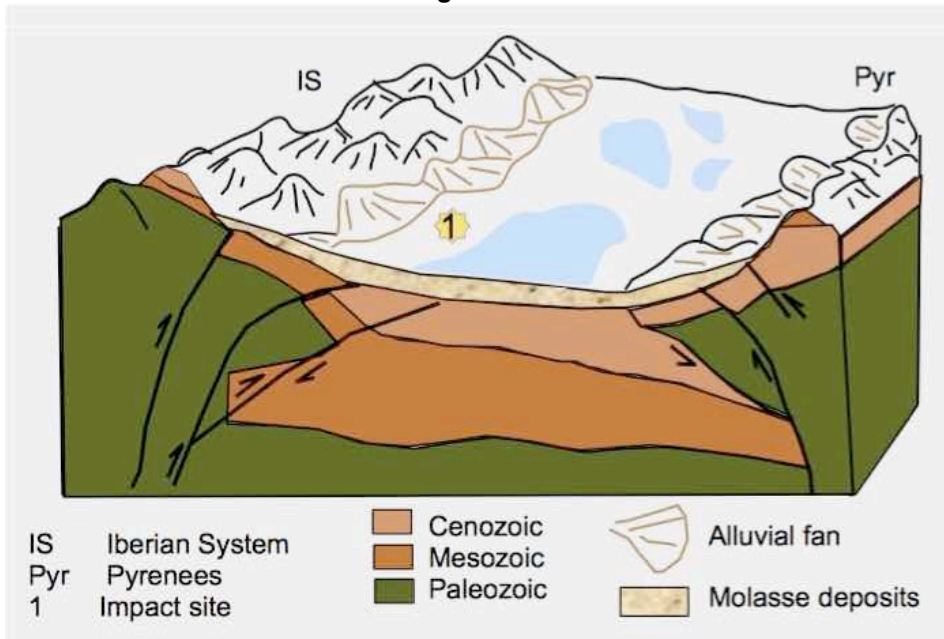


Fig. A102. Cross section of the Azuara impact zone. At the time of impact, the target rocks were made up of Paleozoic, Mesozoic, Cenozoic materials and extensive molasse deposits accumulated at the foot of the reliefs of the Iberian mountain range in emergence.

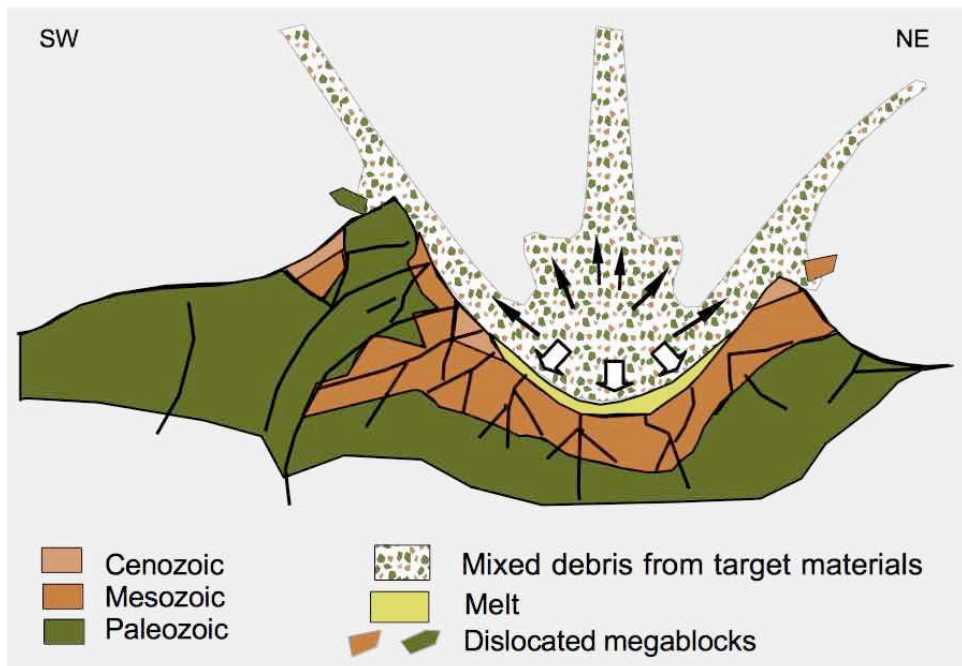


Fig. A103. Shortly after the impact (contact and compression stage): A shock wave compresses the materials of the target in a first phase and then - after release - fragments and ejects them (excavation stage). A curtain of ejecta develops, including megablocks, and comprises all molasse materials removed. Due to the pre-impact geologic setting (Fig. A102) Paleozoic and Mesozoic materials predominate over Cenozoic materials ejected to the southwest. On the NE side, Mesozoic and Cenozoic materials predominate. In the fractures developed in the walls and floor of the crater, materials generated during the impact (impact melts and breccias) are injected giving rise to the formation of breccia dikes.

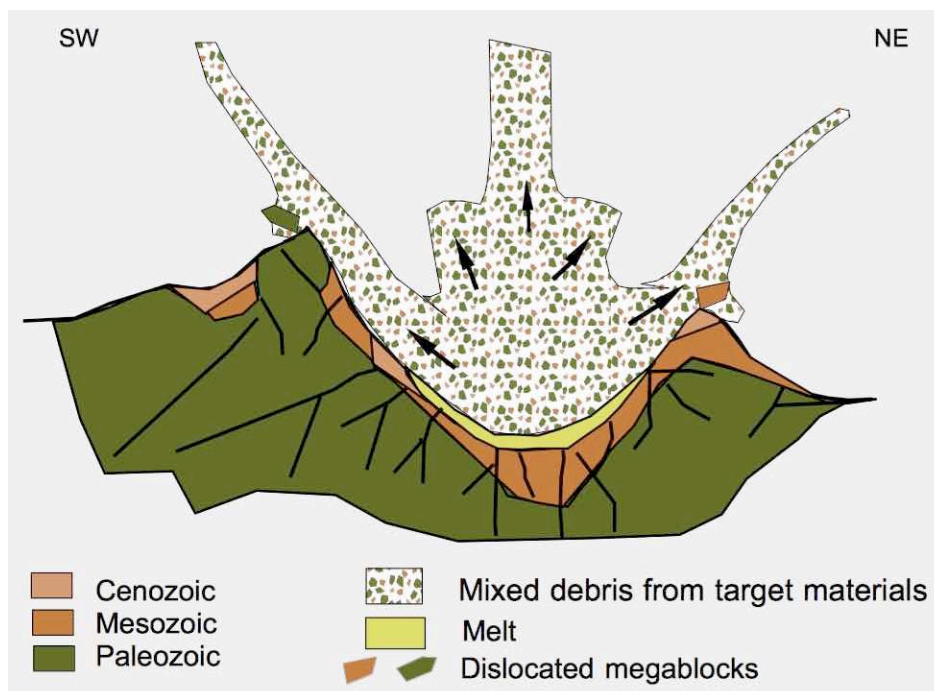


Fig. A104. The ejecta curtain is advancing, with increasing primary crater. In the central part an ejecta plume grows progressively, accompanied by a conical zone of ejecta between plume and ejecta curtain.

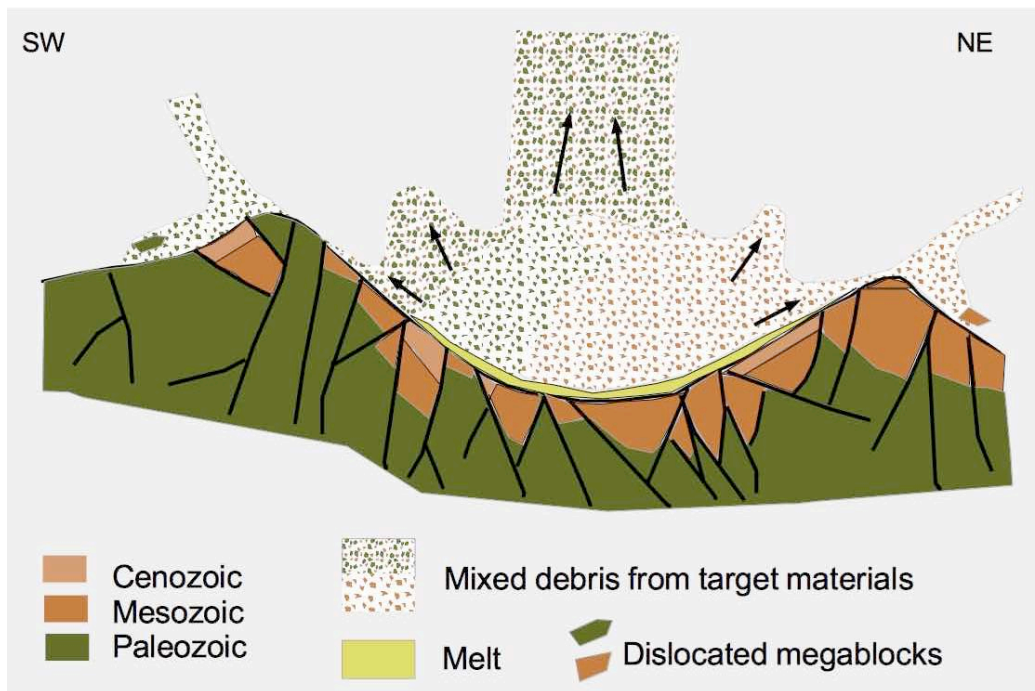


Fig. A105. Progressive growth of the crater to become the transient crater, advance of the ejecta curtain, and increase of ejecta plume and conical zone.

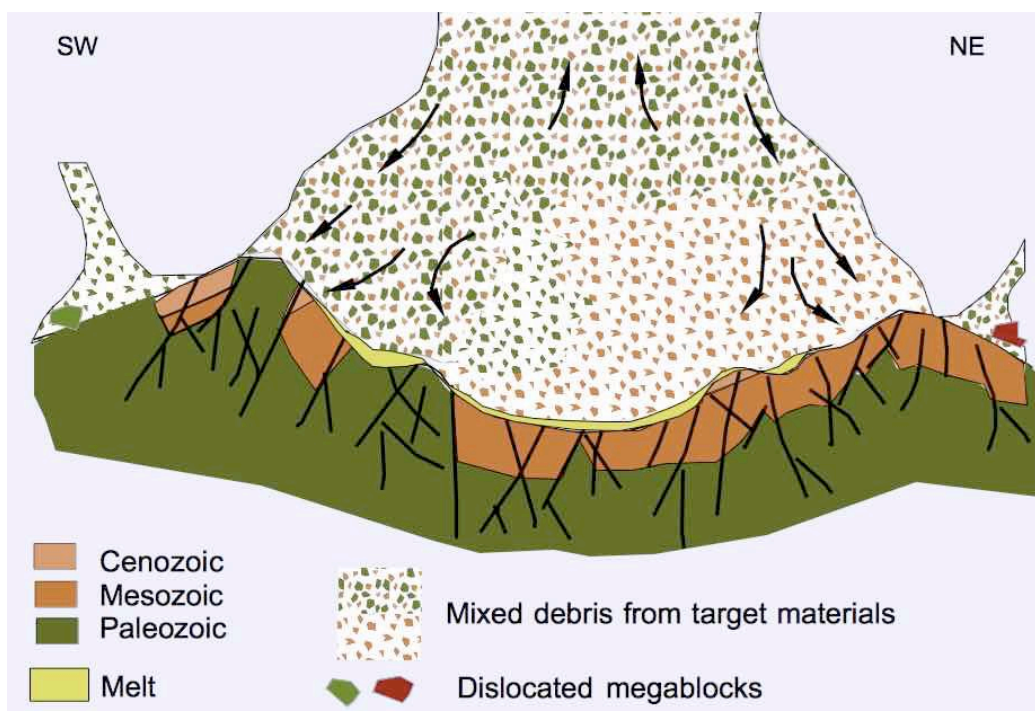


Fig. A106. Modification stage: An inner ring begins to form, further expansion of plume and conical zone. The ejecta of the latter zone begin to leave the crater giving rise to the intracrater gap (Fig. A107).

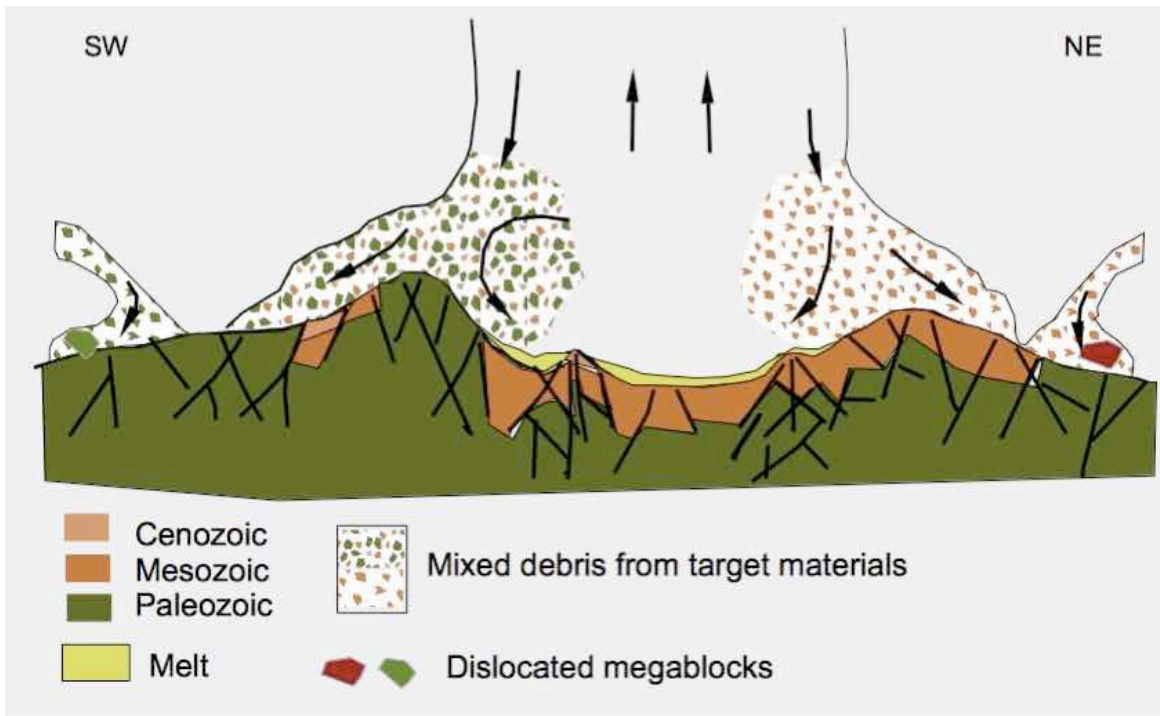


Fig. A107. The materials of the conical zone continue to advance from the intracrater gap. In the case of the SW flank they will give rise to the Pelarda Fm.

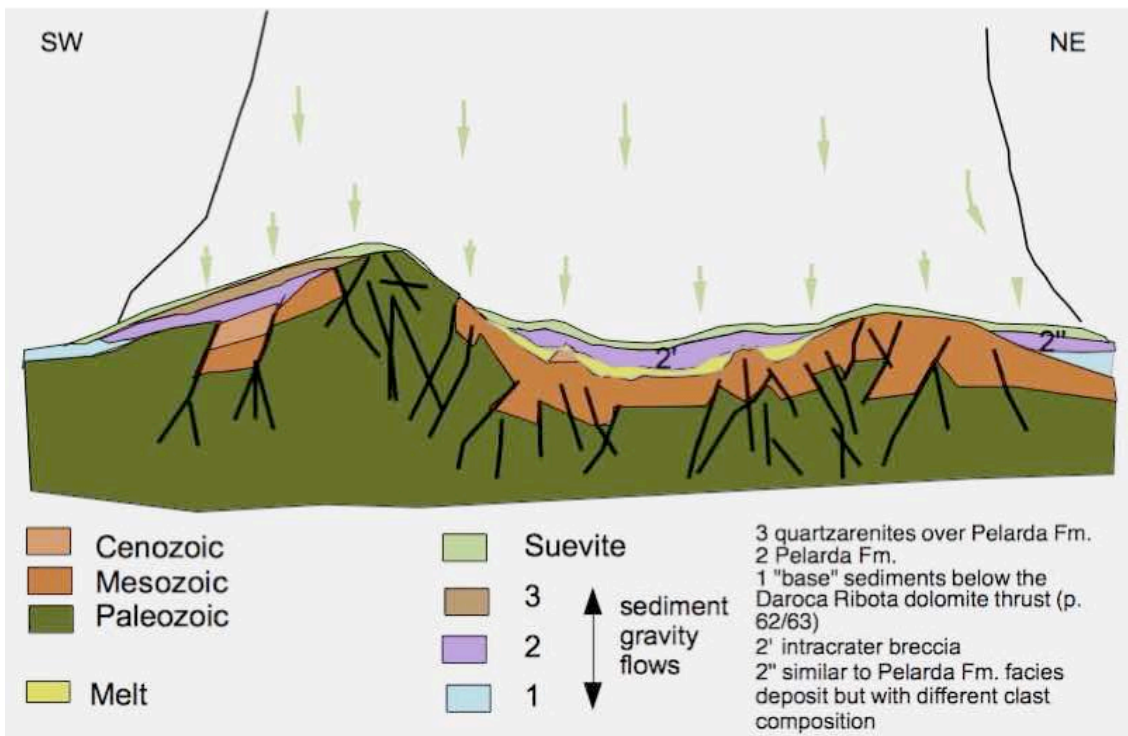


Fig. A108. Materials from the central plume and conical zone begin to deposit to form a breccia of Pelarda Fm. facies within the crater and layers of suevite, which e.g., can still be observed in Cucalón and near Olalla, and which cover all ejecta previously deposited in the Azuara zone.

Appendix II: The Ermita de San Roque Pelarda Fm. ejecta deposit

Near the Aldehuela de Liestos village, 50 km west of Olalla (Fig.1) on top of a distinct hill emerging roughly 100 m from the plain, a peculiar deposit is observed to overlay Eocene (Oligocene) sediments (according to the geological map; Figs. 2, 3). The 5 m thick deposit bears all aspects of the Pelarda Fm. as shown in the images below. The deposit is composed of uncemented, very badly sorted, mostly (more than 95 %) Paleozoic material with well-rounded, subrounded and angular clasts. The main mass is Armorican quartzite, and a few Cretaceous/Jurassic limestone boulders are intermixed. Bámbolea quartzite like in our classic Pelarda Fm. deposit is not observed.

Typical deformations of the clasts occur in the form of spallation fractures; Hertzian fracture cones, distinct small impact imprints and squeezed cobbles.

The deposit is found right in the middle of Mesozoic and Cenozoic sediments; Paleozoic is not exposed within a radius of 10 km at least. On cursory inspection, no quartzite blocks of the size of the San Roque deposit have been observed in the plains around the hill.

We conclude that the San Roque deposit with all aspects of the Pelarda Fm. is suggested to be also ejecta of the Azuara impact event that survived erosion. Alternative explanations for the deposition are meeting serious difficulties.

The considerable distance of about 40 km to the Azuara/Rubielos de la Cérda rims is not a problem at all comparing the figures with the Ries crater ejecta that in the form of limestone blocks (so-called Reuter blocks) can be found up to 60 km distance. In one case one has found a several tons big strongly shattered limestone block in a gravel quarry about 150 km (!) distant from the Ries crater. This block is also interpreted as ejecta although also an origin from Miocene volcanism has been discussed despite the complete lack of any volcanic concomitant material. As for these distal ejecta we must not forget that the Ries is much smaller than Azuara/Rubielos. Possibly in both cases the large ejecta distances may be explained by the spall plate mechanism (Melosh 1989).

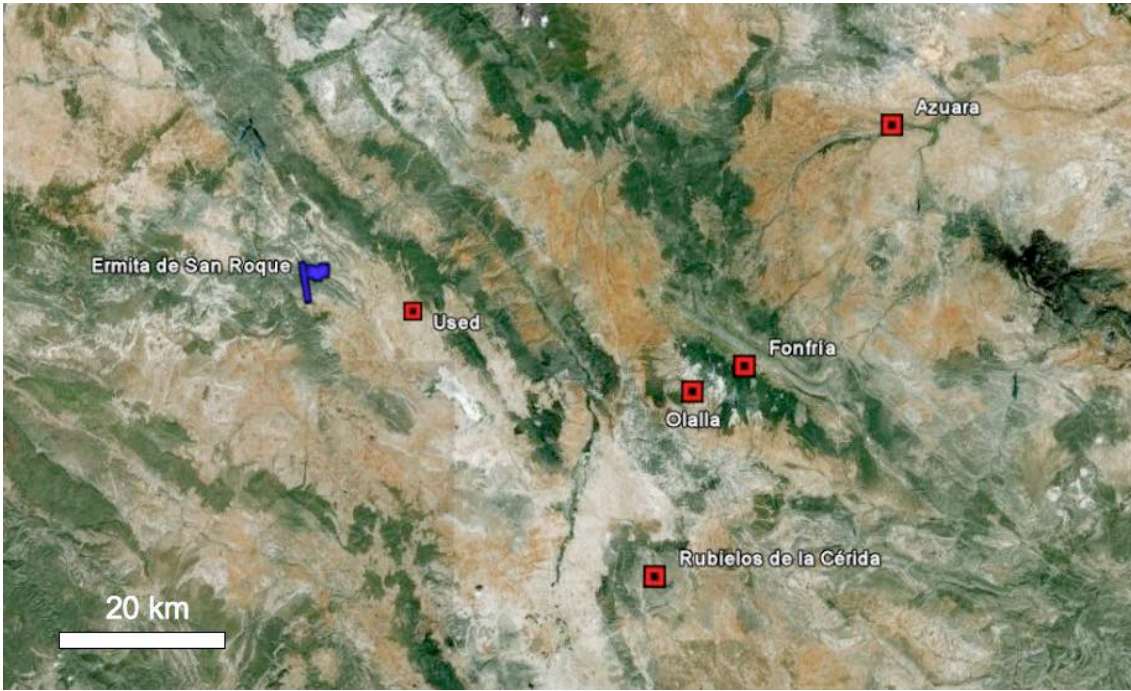


Fig. A201. Location map for the deposit at Aldehueta de Liestos (Ermita de San Roque) west of the villages of Azuara, Fonfría and Olalla.

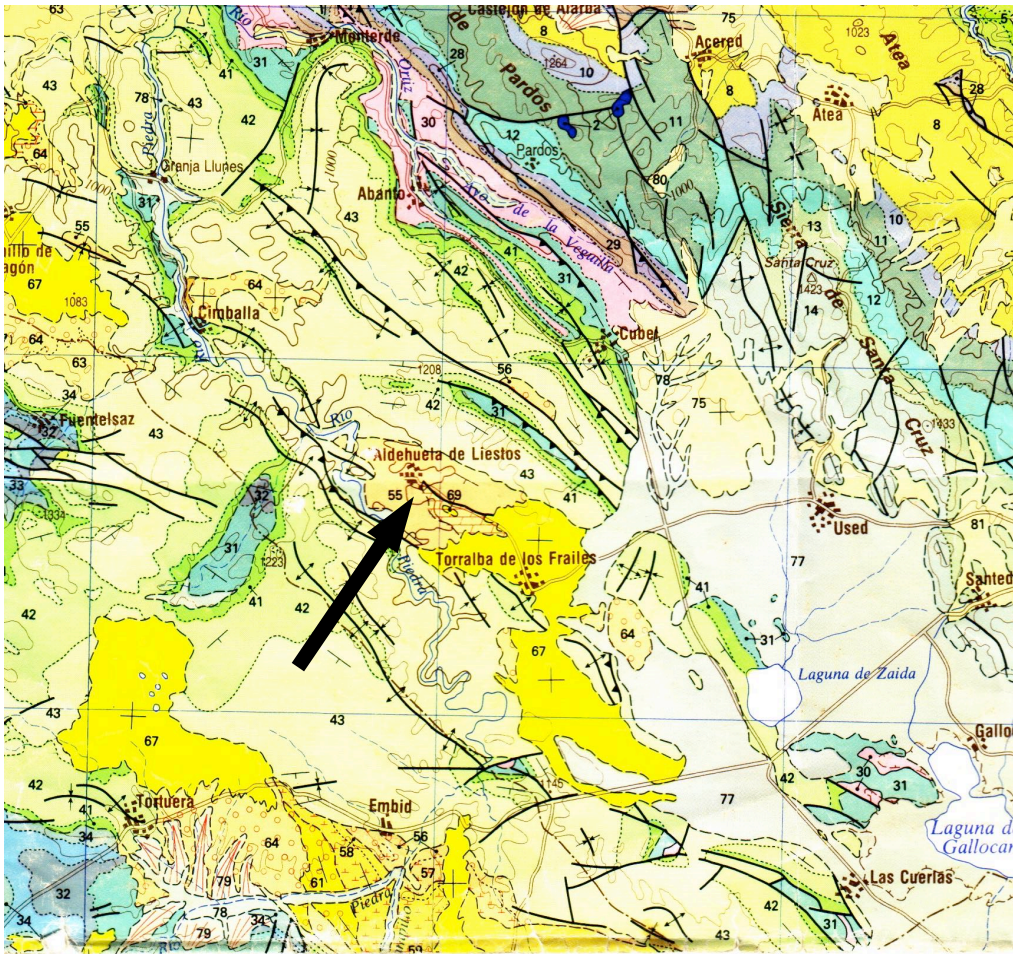


Fig. A202. Geological map of the Ermita San Roque (arrow) area.



Fig. A203. The Ermita de San Roque hill and the geological situation of the Pelarda Fm. deposit. Google Earth oblique view.

In the following we show typical images taken on the Ermita de San Roque hill:

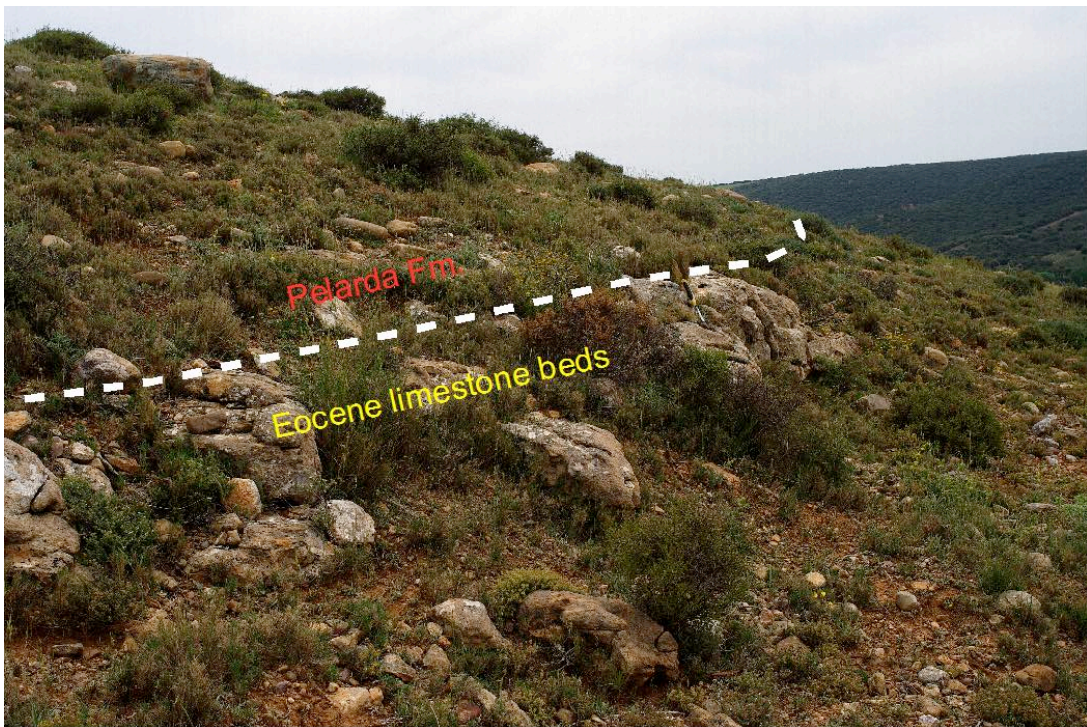


Fig. A204. Pelarda Fm. deposits over autochthonous Eocene limestone beds.



Fig. A205. Closer view of the contact.



Fig. A206. View downhill from the outcropping Eocene limestone beds (lower left corner) to the southwest. The large blocks are Armorican quartzite. Note that downhill the blocks rarefy.



Fig. A207. Aspect of the outcropping Pelarda Fm. The hammer is lying on one of the rare Jurassic/Cretaceous limestone blocks. The outcrop wall is about 3 - 4 m.



Fig. A208. Aspect of the Pelarda Formation. in the field.



Fig. A209. Aspect of the Pelarda Fm. in the field. The larger blocks have obviously been removed by the farmer.

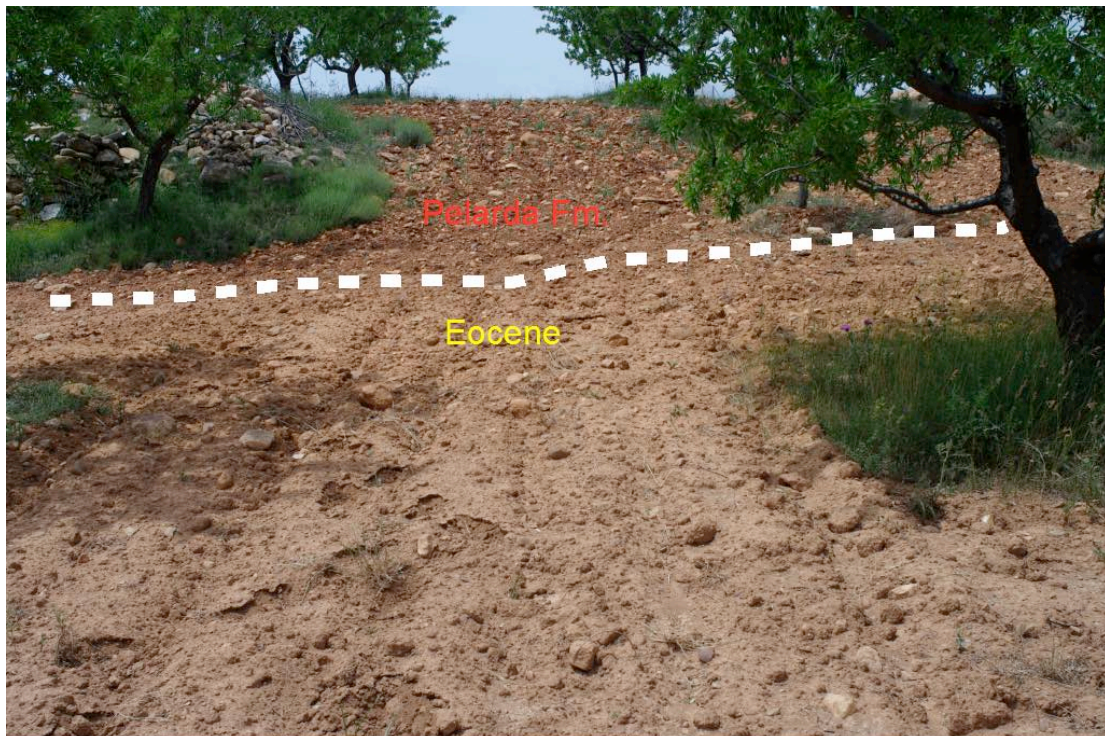


Fig. A210. Mapping the Eocene - Pelarda Fm. boundary in the field.



Fig. A211. Assemblage of Pelarda Fm. clasts. To the right of hammer: Jurassic/Cretaceous limestone boulders. The lowermost quartzite clast shows distinct spallation fractures.



Fig. A212. Large Armorican quartzite block exhibiting irregular fracture and spallation features.

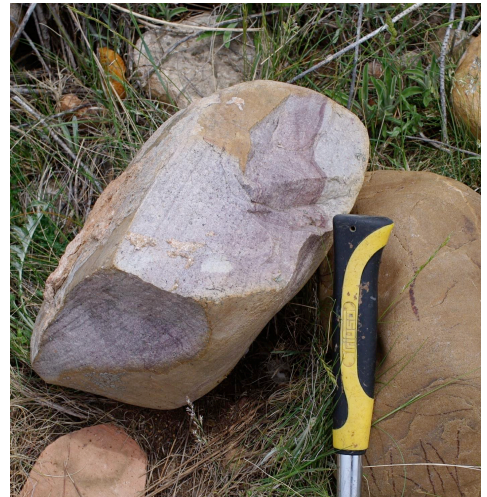


Fig. A213. More spallation fractures.



Fig. A214. Strongly squeezed however coherent quartzite cobble.



Fig. A215. Large quartzite block with distinct concussive marks. Close-up in Fig. 16.



Fig. A216. Close-up of concussion mark with Hertzian fracture cone - arrow head in the center.



Fig. A217. Concussion (spallation) crater in a quartzite block.



Fig. A218. Ermita San Roque built of impact ejecta (except for door and window curbs). This Ermita nicely meets the Ries and Rochechourt impact structures where Impact ejecta have intensively been used as building stones.